

を確認した。暴露測定法および動態解析では、フラーレンのラットへの強制単回経口投与と、MWCNTの気管内投与による生体試料での定量的な検出が可能であることを確認した。*in vitro*試験法の研究においては、リポソーム懸濁フラーレンの暴露により、小核誘発性、神経細胞機能蛋白質に対する影響、Caco-2細胞を使った細胞透過性、マクロファージ細胞からのサイトカイン放出に関して、特に強い影響が見られなかったことを確認してきた。国際動向調査においては、OECDに設置されたワーキンググループ内での討議で、加盟各国でのボランタリーな初期評価研究を進めることが合意されており、本研究班の成果も積極的に取り入れていくべきことが示された。

これらの研究成果をとおして、MWCNTの吸入暴露システムや生体内検出法や*in vitro*試験法のための基礎的技術を確立することを可能にすると共に、MWCNT腹腔内投与での繊維状粒子として観察された事象や気管内投与による発がんプロモーション作用の結果により、*in vivo*長期暴露研究の必要性を強く示すことができたと考えている。

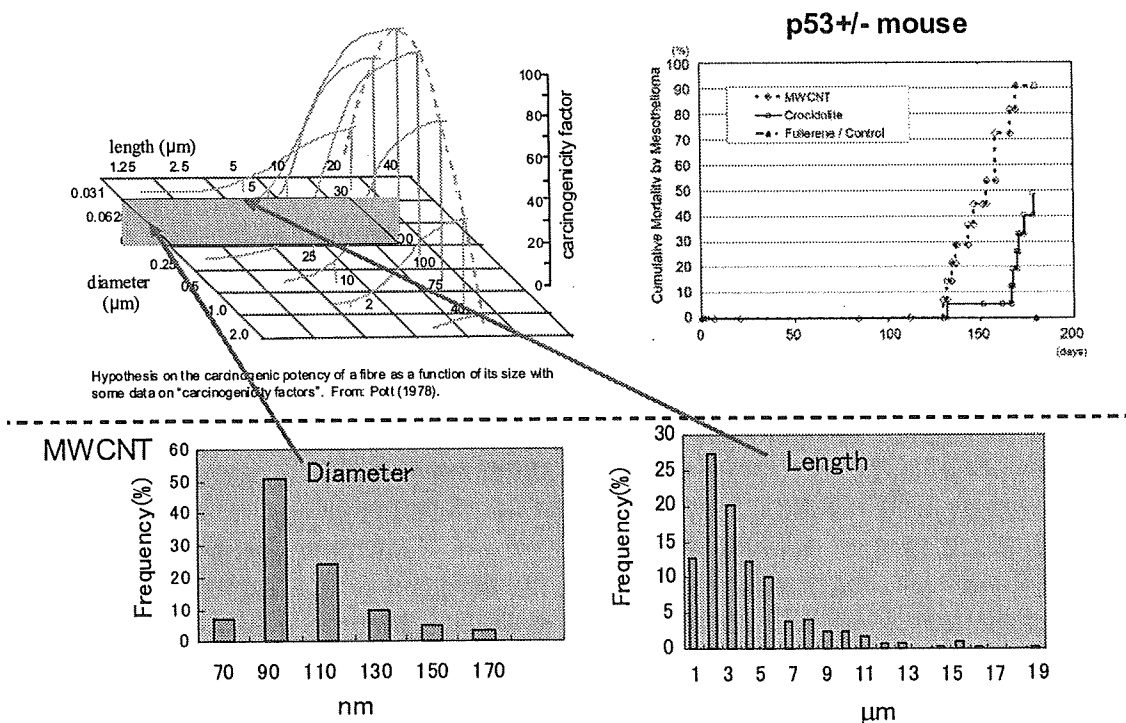
アスベスト様サイズの繊維状粒子の腹腔内投与試験の妥当性

我々のMWCNT腹腔内投与研究を含めて、最近報告されている様々な長さを持つカーボンナノチューブ類の中皮腫誘発性研究については、アスベスト様の繊維状粒子

に関する過去の研究を参考としてデザインされている。ここでは、これらの研究が行われた理由を説明するために、まず過去の経緯についての概説を行う。

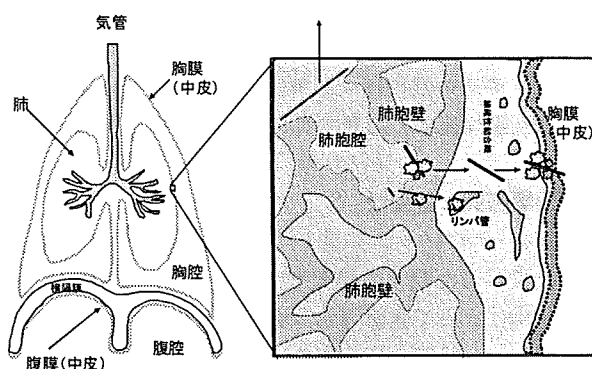
アスベストなどの繊維状粒子の吸入暴露による肺発がん性ポテンシャルは、繊維径と長さおよび体内残留性に依存することが知られている。Davis(1989)ら³²⁾のラットを使った吸入実験では、20 μ m以上の繊維数の多いクリソタイルでアスベスト線維症と発がん性が強くなる傾向が示唆された。それまでの様々な治験をもとにPott(1978)³³⁾は、繊維系と繊維長を関数として発がんポテンシャルの強さを示す仮説を提唱した(図2)。一方、アスベストによる実験動物による中皮腫の誘発は、最初にラットへの胸腔内へのアスベスト埋入実験によって、Wangerによって証明された。さらに、Stanton(1981)ら³⁴⁾による様々な径と長さの分布を持つアスベストを含む鉱物系繊維を胸膜に埋入した実験により、径が1.5 μ m以下で、長さが4 μ m以上の繊維の割合が多いものが、発がん性の強いことが示唆されている。これらの知見をもとに、WHO(1986)³⁵⁾では、繊維長、径および化学組成は体内での沈着、クリアランス、移動に重要な因子であり、胸腔内あるいは腹腔内へ直接投与して中皮腫を誘発させる一連の研究結果からは、繊維長と径が主要な因子であるとした。

図 2. 腹腔内投与による中皮腫誘発作用の検討



この形状に依存した繊維性粒子の発がん性などの慢性影響は、肺の中での体内残留性に関連していると考えられている。WHOでは、PCOMサンプラーでカウント可能な、繊維長5 μm 以上で、繊維径が3 μm 以下で且つ、繊維長:繊維径のアスペクト比3:1以上の粒子 (WHO fiber) を、職域環境でのモニター粒子として推奨してきた。これは、繊毛のある気道を通り抜けて、胚胞まで到達できる粒子 (respirable)は空気力学的な繊維径が5 ~ 10 μm 以下とされているが、繊維長は空気力学的な繊維径に影響を与えないことが示されている^{36, 37)}ことや、5 μm 以上の大きさの繊維は、マクロファージで除去するには大きすぎることによるものであると解釈されている。その結果、これらの繊維状粒子の肺胞域への到達性と、生理学的な難除去性が、繊維長の長い繊維の有害性を示す根拠の一つであると考えられている (図3)。

図3. 繊維状粒子の肺胞域への到達性と生理学的難除去性



アスベストや鉱物系の繊維以外の人工的なガラス質繊維を用いた試験でも、繊維長に依存した発がんポテンシャルを示す結果が得られている。しかし、同じ形状を持つ繊維でもその化学組成の違いで、発がん・慢性影響に違いがあることが示された。また、アスベストの一種クリソタイル (白石綿) も不純物の少ないものは、クロシドライトやアモサイトよりも、繊維数あたりの催腫瘍性が弱いことが知られている³⁸⁾。化学組成の内、鉄原子が、活性酸素発生に強く関わっており、発がん機序の因子と考えられている。実際、クリソタイルを含めたアスベストや人工ガラス質繊維の不純物としても混在している。しかし、その混在量は、同じ物質でもサンプルごとに異なるほか、どのタイプの鉄原子が発がん性に関わっているかは依然不明であり、鉄の混在量と活性酸素の発生量に明らかな相関関係は認められていない³⁹⁾。鉄含量は中皮腫誘発の増強要因であるが、絶対要因ではない。

一方、体内残量性は慢性影響に関して、形状因子 (繊維長と径) の以外に他に最も重要であると認識されてい

る因子としては、化学組成に基づく繊維の体内での耐久性 (durability) が知られている⁴⁰⁾。形状的には、体内残留性が高いと思われる形状の物質でも、長期間体内に残留している間に、粒子表面の収縮や侵食などにより、繊維が分解されたり短くなったりすることにより、物質の組成によっては、肺胞内から除去されていくメカニズムのあることが示唆されている。実際、肺内からの繊維 (特に繊維長の長い (20 μm 以上) 繊維) の排出半減期の長さが、肺への障害性と相関していることが、人工ガラス質繊維を用いた研究で示されている⁴¹⁾。一方、腹腔内投与による中皮腫の誘発の強さも、繊維長の長い繊維の肺からの排出半減期の長さによく相関していることが示されている⁴²⁾。1997年のECのガラス性繊維の有害性物資の分類、包装、表示に関する指定 (EC Commission directive 97/69/EC)⁴³⁾の中では、上記のような知見を受けて、腹腔内投与あるいは吸入試験での発がん性試験での知見に加えて、20 μm 以上の繊維の肺からの消失半減期 (吸入の場合10日、気管内投与の場合40日より短い場合は発がん物質としての表示から除外している) を基準として採用している。

最近のアスベスト代替繊維の評価に関するWHO/IPCSの2005年のワークショップ (WHO Workshop on Mechanisms of Fibre Carcinogenesis and Assessment of Chrysotile Asbestos Substitutes. 8-12 November, 2005, Lyon, France) でもサマリーレポートのなかで、

「物理化学的性質として、化学組成は、繊維の構造と物理化学的性質 (表面積や表面活性) を決定する主要因子であり、繊維粒子成分から発生するフリーラジカルはDNA障害や変異原性を引き起こす。また、繊維表面の物理化学的性質は炎症反応を決定する因子となる。また、繊維の半径・長さや蓄積性に関しては、繊維の長さに依存して生体内残留性が大きくなれば、繊維粒子による発がん性が強くなる傾向にあるとされているが、これはガラス製の繊維によって確認されている事項であり、他の種類の繊維状粒子でも証明されている訳ではない。」

という有害性評価に関するコメントが参加者によるコンセンサスとしてまとめられている。

以上のようにこれまで繊維状粒子と中皮腫の誘発能に関しては、繊維の径と長さ、構成成分、生体内半減期等様々な因子を用いた数多くの研究がなされてきており、アスベストとガラス性繊維に関してはある程度のコンセンサスが得られているものの、繊維性粒子全体の評価としては、依然、明確な国際的コンセンサスは確立していない状況である。しかし、frustrated phagocytosisを仮説とし、組成に関わらず粒子のサイズと形状を重視する考

えも否定されていない。

合成有機繊維やカーボンナノチューブ等の新しい素材の繊維性粒子に関しては、上記のような知見が当てはまるかどうかについては確認の必要性が提言されていた⁴⁴⁾。そこで、我々の研究班では、炭素原子が主成分であるカーボンナノチューブについて、その形状（繊維長や径）から予想される中皮腫誘発能を検証することとした。

繊維長の長いタイプのMWCNTの腹腔内投与試験の結果

我々の研究で使用した多層カーボンナノチューブ(MWCNT)について、その繊維径と長さを測定したところ図2の結果を得ている。これらの大きさは、初期に提唱された発がんポテンシャルを示す大きさのレンジと重なることが示された。その発がん性を評価するにあたり、暴露経路を考慮すると吸入暴露による実験が適切であるとは考えられたが、カーボンナノチューブは、凝集しやすい性質を持っており、研究班がスタートした直後においては、液体等に分散するなどして気管内投与を行うことを念頭においても、適切に分散して投与/吸入暴露を行う手法が存在していなかった。また吸入暴露による検証の必要性についても、論議の分かれるところであり、過去の吸入暴露実験による齧歯類の発がん感受性が人のそれに対して著しく低く、発がんポテンシャルを過小評価する可能性、そして、むしろ齧歯類における腹腔内投与結果との対応の方が、人における発がんポテンシャルを正當に評価するのではないかと指摘もあるため、上述した腹腔内投与法の妥当性に鑑み、最初の試験の暴露経路として検出力の高い腹腔内暴露を選定した。しかし、最も発がんポテンシャルの強いアスベスト（クロシドライト）を用いた腹腔内投与研究でも、中皮腫の誘発には、1年以上の期間が必要であることが知られていたため、より短期間での検出法を検討した。その結果、P53(+/-)ヘテロノックアウトマウスを使った腹腔内投与手法により、アスベストによる中皮腫誘発を約半年まで短縮できる研究が報告^{45, 46)}されており、この手法を用いてナノチューブとフラーレンを検討することとした。P53(+/-)マウスを用いたオリジナルの手法では、200 μ g (5.8 $\times 10^8$ fibre) を週に一回35週間腹腔内投与しているが、複数回投与による繊維長非依存的な毒性を回避するために単回投与で行うこととした。また、未だ最終化はされていないが、1997年にECのEuropean Chemical Bureauの合同研究センター (Joint Research Center) で作成されたManMadeMineralFibres (MMMF) 試験法のドラフト案⁴⁷⁾では、繊維数として1 $\times 10^9$ WHO fiber/ratの単回投与を標準としている。また、Rollerら (1997)⁴⁸⁾の様々な繊維粒子を腹腔内投与した際の用量（繊維数）依存性からは、10⁹ fiber/animal程度を投与すれば、様々な繊維で

の中皮腫の発生を捉え得ることが示されている。研究結果としては、p53のヘテロノックアウトマウスに3mg/miceを腹腔内単回投与した場合に、投与後半年までの間に、ほとんどのマウスに中皮腫の発生が認められた³⁰⁾。(尚、現在解析中の追加試験では、1000分の一の用量である3 μ g/mouseの腹腔内投与でも、中皮腫の発生することを確認している)。同時に投与したクロシドライト (3mg/mice) においても、ほとんどのマウスに中皮腫を誘発したが、未修飾フラーレンを同用量 (3mg/mouse) 投与した場合は、対象群と同様に中皮腫の発生を認めなかった。

ほぼ同時期に発表された別の研究では、長さの違う4種類のMWCNTを50 μ g/kgの用量で腹腔内単回投与して、7日後の中皮細胞の増殖性を検証したところ、長いタイプの2種類について腹腔側にCNTを取り込んだ群においてのみ細胞が集合した肉芽の形成が認められた²⁹⁾。この結果は、我々の結果を支持する結果である⁴⁹⁾。さらに、我々が用いた長いタイプのMWCNTは、野生型のラットを用いた腹腔（陰嚢腔）内投与研究によっても、中皮腫を誘発する能力を持つことが明らかにされた³¹⁾。尚、短いタイプやその他の様々な形状のMWCNTにおける慢性毒性は別途検証する必要がある。

慢性影響研究の重要性

p53のヘテロノックアウトマウスにナノマテリアルを腹腔内投与した我々の研究では、分散したMWCNT繊維が食細胞によって貪食された像として認められ、繊維を含んだ細胞が腹膜の病変部のみならず肝類洞内又は肝葉間の線維性中隔に沿って及び腸間膜リンパ節の中にも認められることが示されている。また、中皮腫誘発性を示さなかったフラーレンについては、腹膜において小さな暗褐色斑を漿膜表面に認めるのみであったが、この暗褐色斑は投与したフラーレン凝集塊のサイズと形が一致しており、その裂隙の辺縁が褐色に染まった像が捕らえられている。これは、食細胞によるフラーレン粒子の表面の生体による細分散の可能性を示唆しているものと推定された。この実験を再解析した結果、フラーレン投与群において、体重増加抑制、腎の巣状萎縮、組織学的に尿細管上皮の空胞変性（PAS染色陰性、脂肪染色陰性）～尿細管の萎縮と円柱形成によるネフロン萎縮ないし脱落が誘発されていることが示唆され、現在、追試による確認を進めている。少なくともフラーレン凝集体が貪食細胞等により細粒化され、全身に再分布して影響を引き起こした可能性が示唆された。

以上のことは、アスベスト様の繊維状粒子の慢性暴露による中皮腫誘発性だけでなく、体内に取り込まれ得るサイズのナノマテリアルの長期体内残留とそれに対

する生体反応の様式が、慢性的に身体に大きく影響することを示唆しており、ナノマテリアルの未知の生体影響を検索していくための慢性影響研究は、より重要な研究テーマとして取り上げるべきであると考えられる。

おわりに

産業用ナノマテリアルはナノテクノロジーの中心的な新規物質として、近年急速にその種類や生産量が増加しつつあるが、産業用途として期待されている物理化学特性は、同一化学組成を持つ大きな構造体とは異なる生理活性やヒト健康影響に対する懸念をもたらす可能性を含んでいる。このような懸念に対して、ナノマテリアルの特性を考慮した有害性評価手法の開発と評価の実施が急務となっており、我々は、本問題に対処するための体内動態モニタリング法、*in vitro*及び*in vivo*の評価法開発の為に基礎的研究を進めてきたところである。ナノマテリアルによる健康影響評価法について論点の整理では、基本的な評価概念については、従来の化学物質と同様であると考えられものの、ナノマテリアル特有の物理化学的性状のため、特に分散法や体内蓄積性といった観点で新しい技術の導入や手法開発が必要であることが示された。一方、ナノマテリアルの想定された体内動態に従い最も懸念された慢性影響として、繊維状粒子による中皮腫形成について、アスベスト同様の大きさや形の繊維を含むカーボンナノチューブが腹腔内投与試験よりそのポテンシャルを持つことを明らかにしてきた。加えて、この研究は短い繊維状のナノチューブやフラーレンが、細胞による食作用等を介して体内に再分布する可能性を示唆した。これらのことは、ナノマテリアルの長期体内残留とそれに対する生体反応の様式が、慢性影響に大きく影響することを示唆すると共に、表面活性の高いナノマテリアルと体内成分（細胞を含む）との基礎的な相互作用、体内残留様式、及び慢性有害性影響の同定が、ナノマテリアルの健康影響評価研究の中で最も重要な検討事項であることを示したものであると考えている。多くの点で未確定の部分が多いナノマテリアルの健康影響評価において、*in vitro*及び*in vivo*の評価などの様々なアプローチが必要であることに異論の余地はないところである。しかし、闇雲にあらゆるエンドポイントやスクリーニング手法の検証を進めることより、回り道のようにみえるかもしれないが、想定される重要な*in vivo*影響を同定し、その影響の発現メカニズムや検出マーカーを検索しながら評価手法を整備していくことの方が、より早く評価手法の確立に繋がるのではないかと考えている。

1) SCENIHR (Scientific Committee on Emerging and Newly Identified Health Risks), The appropriateness

of existing methodologies to assess the potential risks with engineered and adventitious products of nanotechnologies. Adopted during the 10th plenary 26 March 2006 after public consultation. SCENIHR 002/05 (2006).

- 2) SCENIHR (Scientific Committee on Emerging and Newly Identified Health Risks), Opinion On The Appropriateness Of The Risk Assessment Methodology In Accordance With The Technical Guidance Documents For New And Existing Substances For Assessing The Risks Of Nanomaterials. Adopted during the 19th plenary 21-22 June 2007 after public consultation (2007).
- 3) FSA (Food Safety Authority of Ireland), The Relevance for Food Safety of Applications of Nanotechnology in Food and Feed (2008).
- 4) COT, UK Committees on toxicity, mutagenicity and carcinogenicity of chemicals in food, consumer products and the environment (COT, COM, COC). Joint statement on nanomaterial toxicology (2005).
- 5) COT, UK Committee on toxicity, of chemicals in food, consumer products and the environment. COT Addendum to joint statement of the Committees on toxicity, mutagenicity and carcinogenicity of nanomaterial toxicology. COT Statement 2007/01, March 2007 (2007).
- 6) Lee, K.P. Trochimowicz, H.J. and Reinhardt, C.F.:Toxicol. Appl. Pharmacol. 79, 179-92 (1985)
- 7) IARC:IARC Monogr Eval Carcinog Risks Hum. 46, 1-458 (1989)
- 8) IARC. Summaries and Evaluation. Carbon Black, Titanium Dioxide and Non-Asbestiform Talc. 2006; Available from: <http://monographs.iarc.fr/ENG/Meetings/93-titaniumdioxide.pdf>.
- 9) Donaldson, K. Stone, V. Clouter, A. Renwick, L. and MacNee, W.:Occup. Environ. Med. 58, 211-6, 199 (2001)
- 10) Oberdorster, G. Maynard, A. Donaldson, K. Castranova, V. Fitzpatrick, J. Ausman, K. Carter, J. Karn, B. Kreyling, W. Lai, D. Olin, S. Monteiro-Riviere, N. Warheit, D. and Yang, H.:Part Fibre Toxicol. 2, 8 (2005)
- 11) Warheit, D.B. Webb, T.R. Sayes, C.M. Colvin, V.L. and Reed, K.L.:Toxicol. Sci. 91, 227-36 (2006)
- 12) Warheit, D.B. Webb, T.R. Reed, K.L. Frerichs, S. and Sayes, C.M.:Toxicology. 230, 90-104 (2007)
- 13) Lademann, J. Weigmann, H. Rickmeyer, C.

- Barthelmes, H. Schaefer, H. Mueller, G. and Sterry, W.:*Skin Pharmacol. Appl. Skin Physiol.* 12, 247-56 (1999)
- 14) Pflucker, F. Wendel, V. Hohenberg, H. Gartner, E. Will, T. Pfeiffer, S. Wepf, R. and Gers-Barlag, H.:*Skin Pharmacol. Appl. Skin Physiol.* 14 Suppl. 1, 92-7 (2001)
- 15) Kreilgaard, M.:*Adv Drug Deliv Rev.* 54 Suppl. 1, S77-98 (2002)
- 16) Sera, N. Tokiwa, H. and Miyata, N.:*Carcinogenesis.* 17, 2163-9 (1996)
- 17) Baierl, T. Drosselmeyer, E. Seidel, A. and Hippeli, S.:*Exp Toxicol. Pathol.* 48, 508-11 (1996)
- 18) Sayes, C. Fortner, J. Guo, W. Lyon, D. Boyd, A. Ausman, K. Tao, Y. Sitharaman, B. Wilson, L. Hughes, J. West, J. and Colvin, V.:*Nano Lett.* 4, 1881-1887 (2004)
- 19) Isakovic, A. Markovic, Z. Todorovic-Markovic, B. Nikolic, N. Vranjes-Djuric, S. Mirkovic, M. Dramicanin, M. Harhaji, L. Raicevic, N. Nikolic, Z. and Trajkovic, V.:*Toxicol. Sci.* 91, 173-83 (2006)
- 20) Sayes, C.M. Marchione, A.A. Reed, K.L. and Warheit, D.B.:*Nano Lett.* 7, 2399-406 (2007)
- 21) Moriguchi, T. Yano, K. Hokari, S. and Sonoda, M.:*Fullerenes, Nanotubes and Carbon Nanostructures.* 7, 195 - 209 (1999)
- 22) Moriguchi, T. Yano, K. Hokar, S. and Sonda, M.:*Fullerene Science and Technology.* 7, 195-209 (1999)
- 23) Warheit, D.B. Laurence, B.R. Reed K, L. Roach, D.H. Reynolds, G.A.M. and Webb, T.R.:*Toxicological sciences : an official journal of the Society of Toxicology.* 77, 117-125 (2004)
- 24) Lam, C.-W. James, J.T. McCluskey, R. and Hunter, R.L.:*Toxicological sciences : an official journal of the Society of Toxicology.* 77, 126-134 (2004)
- 25) Shvedova, A.A. Kisin, E.R. Mercer, R. Murray, A.R. Johnson, V.J. Potapovich, A.I. Tyurina, Y.Y. Gorelik, O. Arepalli, S. Schwegler-Berry, D. Hubbs, A.F. Antonini, J. Evans, D.E. Ku, B.-K. Ramsey, D. Maynard, A. Kagan, V.E. Castranova, V. and Baron, P.:*American journal of physiology. Lung cellular and molecular physiology.* 289, L698-708 (2005)
- 26) Li, Z. Hulderman, T. Salmen, R. Chapman, R. Leonard, S.S. Young, S.-H. Shvedova, A. Luster, M.I. and Simeonova, P.P.:*Environmental health perspectives.* 115, 377-382 (2007)
- 27) Muller, J. Huaux, F. Moreau, N. Misson, P. Heilier, J.-F. Delos, M. Arras, M. Fonseca, A. Nagy, J.B. and Lison, D.:*Toxicology and applied pharmacology.* 207, 221-231 (2005)
- 28) Nemmar, A. Hoet, P.H.M. Vandervoort, P. Dinsdale, D. Nemery, B. and Hoylaerts, M.F.:*Journal of thrombosis and haemostasis : JTH.* 5, 1217-1226 (2007)
- 29) Poland, C.A. Duffin, R. Kinloch, I. Maynard, A. Wallace, W.A. Seaton, A. Stone, V. Brown, S. Macnee, W. and Donaldson, K.:*Nat Nanotechnol.* 3, 423-8 (2008)
- 30) Takagi, A. Hirose, A. Nishimura, T. Fukumori, N. Ogata, A. Ohashi, N. Kitajima, S. and Kanno, J.:*J Toxicol. Sci.* 33, 105-16 (2008)
- 31) Sakamoto, Y. Nakae, D. Fukumori, N. Tayama, K. Maekawa, A. Imai, K. Hirose, A. Nishimura, T. Ohashi, N. and Ogata, A.:*J Toxicol. Sci.* 34, 65-76 (2009)
- 32) Davis, J.M.:*IARC Sci Publ.* 33-45 (1989)
- 33) Pott, F.:*Staub, Reinhaltung der Luft.* 38, 486-490 (1978)
- 34) Stanton, M.F. Layard, M. Tegeris, A. Miller, E. May, M. Morgan, E. and Smith, A.:*J Natl Cancer Inst.* 67, 965-75 (1981)
- 35) WHO, ASBESTOS AND OTHER NATURAL MINERAL FIBRES (ENVIRONMENTAL HEALTH CRITERIA 53) (1986).
- 36) Timbrell, V.:*J. Occup. Health Soc. Aust.* 3, 3-12 (1983)
- 37) HSE, An inventory of fibres to classify their potential hazard and risk (2006).
- 38) Bernstein, D.M. Rogers, R. and Smith, P.:*Inhal. Toxicol.* 15, 1247-74 (2003)
- 39) WHO, Consensus report of 'IARC Scientific publication No.140' (1999).
- 40) Bignon, J. Saracci, R. and Touray, J.C.:*Environ Health Perspect.* 102 Suppl. 5, 3-5 (1994)
- 41) Hesterberg, T.W. Chase, G. Axten, C. Miller, W.C. Musselman, R.P. Kamstrup, O. Hadley, J. Morscheidt, C. Bernstein, D.M. and Thevenaz, P.:*Toxicol. Appl. Pharmacol.* 151, 262-75 (1998)
- 42) Bernstein, D.M. Riego Sintes, J.M. Ersboell, B.K. and Kunert, J.:*Inhal. Toxicol.* 13, 823-49 (2001)
- 43) EC:Official Journal of the European Communities, (1997)
- 44) Donaldson, K. and Tran, C.L.:*Mutat Res.* 553, 5-9 (2004)

- 45) Marsella, J.M. Liu, B.L. Vaslet, C.A. and Kane, A.B.:*Environ. Health Perspect.* 105 Suppl 5, 1069-72 (1997)
- 46) Vaslet, C.A. Messier, N.J. and Kane, A.B.:*Toxicol. Sci.* 68, 331-8 (2002)
- 47) ECB, METHODS FOR THE DETERMINATION OF THE HAZARDOUS PROPERTIES FOR HUMAN HEALTH OF MAN MADE MINERAL FIBRES (MMMF) (1999).
- 48) Roller, M. Pott, F. Kamino, K. Althoff, G.H. and Bellmann, B.:*Environ. Health Perspect.* 105 Suppl. 5, 1253-6 (1997)
- 49) Kane, A.B. and Hurt, R.H.:*Nat. Nanotechnol.* 3, 378-9 (2008)

高速液体クロマトグラフィー-タンデム質量分析法による生物試料中フラーレンの分析法の開発

久保田領志[#], 田原麻衣子, 清水久美子, 杉本直樹, 広瀬明彦, 西村哲治Development of a liquid chromatography-tandem mass spectrometry method for the determination of fullerenes C₆₀ and C₇₀ in biological samplesReiji Kubota[#], Maiko Tahara, Kumiko Shimizu, Naoki Sugimoto, Akihiko Hirose, and Tetsuji Nishimura

Wide application of fullerenes in various areas would increase the risk of occupational and environmental exposure to human. However, information about toxicity and biological behavior of fullerenes is not sufficient for the risk assessment at present. For the determination of fullerene C₆₀ in biological samples, an analytical method using high performance liquid chromatography – tandem mass spectrometry (LC-MS/MS) and extraction procedure from tissues of experimental animals was established in this study. Using LC-MS/MS with an atmospheric pressure chemical ionization in negative mode, C₆₀ were identified and quantified. After optimization of mobile phase and separation column, good separation of peak of fullerene and sensitivity were obtained in case of using toluene and acetonitrile as the mobile phases and Develosil RPFULLERENE as the separation column. For method validation, rat brain, kidney, liver, lung, spleen tissues and blood were used for recovery tests. Good results were obtained and the recovery percentages were found to be between 98.1% and 106.5%.

Keywords: fullerene, analytical method, LC-MS/MS, biological Sample, extraction

1. はじめに

近年, ナノテクノロジー素材である人工ナノ粒子 (Engineered nanoparticles, ENPs) は新機能や優れた物理化学的特性を持つことから, 情報・通信, 医療, 環境, エネルギー等の様々な分野において次世代を担うキーテクノロジーとして期待され, 急速に種類や生産量が増加しつつある. 代表的なENPsとしては, カーボンナノ粒子 (フラーレンやカーボンナノチューブ等), 金属・合金・金属酸化物のナノ粒子, ポリマーナノ粒子, 量子ドット等があり, 賦形剤, 乳白剤, 触媒, 半導体等の工業分野だけでなく, ヒトに直接関係する製薬, 食品, 化粧品等の分野においても用いられている¹⁾. 一方で, それらENPsのヒトへの健康影響や環境への放出, 生態系への影響については多くの点で未解明のままであり, 特にENPsによるヒトに対する健康影響評価への関心が高まっているのが現状である^{2,3)}.

カーボンナノ粒子のフラーレンは, グラファイト, ダイヤモンドに次ぐ第三の炭素同素体であり, 他の炭素同素体とは異なる多数の五角面と六角面を持つ閉多面体か

ご型構造の分子である⁴⁾. その独特な構造と特性のためにフラーレンと内包フラーレンや化学修飾フラーレンなどの誘導体は, 他の炭素同素体とは異なりフリーラジカルスカベンジャー⁵⁾, 光誘起DNA切断⁶⁾, HIV-1プロテアーゼ活性阻害⁷⁾, ヒト細胞 (ヒト皮膚線維芽細胞 (HDF細胞), ヒト肝ガン由来細胞 (HepG2細胞), およびヒト星状細胞 (NHA細胞) における細胞毒性⁸⁾を示すことが報告されている. フラーレンとその誘導体の急速な商用化により, ヒトが職業や環境から経口, 経皮, 経気道曝露するリスクが増大することが推測されている. しかしながら, 曝露によるヒト健康への影響は殆ど明らかにされておらず, 有害影響評価や体内動態に関する研究は十分ではない. *in vivo*⁹⁾や*in vitro*¹⁰⁾によるフラーレンやその誘導体の有害影響を正しく評価するためには, フラーレンの曝露評価が不可欠である. そのためには, フラーレンの高感度, 高精度および選択性が高い分析化学的手法が必要である. しかしながら, 分析化学的手法を用いた生物試料中のフラーレンやその誘導体の測定に関する研究は数例あるだけで¹¹⁻¹³⁾, これらの研究を行う上でも, 分析法の開発が急務となっている.

そこで本研究では, 高速液体クロマトグラフィー-タンデム質量分析法 (LC-MS/MS) を用いたフラーレン (C₆₀) の高感度測定法の確立の目的とし, 投与した実験動物の

[#] To whom correspondence should be addressed: Reiji Kubota; Kamiyoga 1-18-1, Setagaya-ku, Tokyo 158-8501, Japan; Tel/Fax.: 03-3700-9346; E-mail: reijik@nihs.go.jp

組織からのフラレン類の抽出等の前処理法を検討した。

2. 実験方法

2.1 試薬

C₆₀はMaterials Technologies Research社製 (Cleveland, USA) (純度99.98% (メーカー成績値)) またはフロンティアカーボン (株) (東京, 日本) 製ナノムパーブルSUH (純度>99.9% (メーカー成績値)) を, C₇₀はMaterials Technologies Research社製 (Cleveland, USA) (純度99.5% (メーカー成績値)) を用いた。高速液体クロマトグラフィー用2-プロパノール, アセトニトリル, およびトルエンは和光純薬工業 (株) (大阪, 日本) 製を用いた。また, 生化学用のドデシル硫酸ナトリウムも和光純薬工業 (株) (大阪, 日本) 製を用いた。標準原液はC₆₀またはC₇₀を10mg精密に量り取り, それぞれトルエン10mLに加え超音波処理および攪拌して溶解したものとし, 分析まで-20℃で保存した。標準液は標準原液からトルエンで段階的に希釈したものを用時調製した。

2.2 装置

LC-MS/MSには, 高速液体クロマトグラフとしてWaters社 (Milford, USA) 製Alliance 2695 HPLCシステムを, タンデム質量分析装置として同社製Micromass Quattro micro APIトリプル四重極質量分析計を連結したものをを用いた。

2.3 LC-MS/MSの分析条件

移動相の最適化は, 以下の2組の条件 (条件1: A1-A2, 条件2: B1-B2) で比較検討した。条件1では, 移動相A1=トルエンおよびA2=2-プロパノールを, A1/A2の割合を27%/73%, 36%/64%および45%/55%に設定した。条件2では, 移動相B1=トルエンおよびB2=アセトニトリルを, B1/B2の割合を50%/50%, 60%/40%および70%/30%に設定した。条件1, 2共にアイソクラティックモードで送液し, 流速は0.2および1.0 mL/minとした。カラムオープンの温度は40℃ (一部30℃も用いた) を用いた。オートサンプラーは10℃で維持し, 注入量は5μLもしくは20μLで行った。

イオン化法は, 大気圧化学イオン化法 (APCI) のネガティブイオンモードを用い, Multiple Reaction Monitoring (MRM) モードにより高感度定量分析を行った。対象物質の分離カラムによる分離条件を比較検討するためにWaters社製 Atlantis dC18 (3 μm, 2.1 × 150 mm) (極性化合物の保持にすぐれ, 100%水系移動相でも使用できるC18系逆相カラム) および 野村化学 (株) (瀬戸, 日本) 製Develosil RPFULLERENE (5 μm, 4.6 × 250 mm) (C18

系) に比べ, 保持が大きく, 高い耐久性を示すC30系逆相カラム) を用いた。LC-MS/MSのシステム制御, データ収集および解析にはWaters MassLynx version 4.0を用いた。

MRM測定条件は, 標準液を直接注入し, イオン検出強度が最大になるように最適化した。以下に条件を示す。APCIのコロナ電流は15μA, ソース温度, APCIプローブ温度はそれぞれ120℃, 400℃を用いた。デゾルベーションガス流量およびコーンガス流量はそれぞれ600L/hr, 50L/hrとした。インタースキャンディレイは0.1secs, インターチャンネルディレイは0.05secsに設定し, ドウエルトタイムは0.5secsを用いた。フラレンのプレカーサイオン, プロダクトイオンについては, C₆₀が $m/z = Q1\ 720 \rightarrow Q3\ 720$, サロゲート物質として回収率補正に用いるC₇₀では $m/z = Q1\ 840 \rightarrow Q3\ 840$ とし, コリジョンエネルギーはC₆₀, C₇₀ともに60eV, コーン電圧は120Vを採用した。

2.4 試料の前処理法

生物試料からのC₆₀の抽出はMoussaら (1997)¹⁴⁾ の方法を簡便化して行った。分析まで冷凍保存していた臓器の重量を測定し, ホモジナイズし, 50~200mgをガラス製のホモジナイズ管に量り取った。これに0.1Mのドデシル硫酸ナトリウム0.5mL, および内部標準物質溶液として1.0mg/L C70トルエン溶液0.5mLを添加し, 穏やかにホモジナイズした。ホモジネートをガラス製の遠沈管に移し, ホモジナイズ管を1.0mLのトルエンで5回洗浄し, その洗液をホモジネートに合わせた。次にホモジネートを合わせた遠沈管に0.5mLの酢酸を加え遮光し, 室温で5時間295/minで振とう後, 30分間3500rpmで遠心した。遠心後, 上澄みを分取し, LC/MS/MS分析用試料とした。

3. 結果と考察

3.1 移動相の最適条件の検討

フラレンの分離における移動相の最適条件を検討した。まず, C18系逆相カラムのAtlantis dC18カラムを用い, 2組の移動相の条件でそれぞれ100μg/LのC₆₀とC₇₀のトルエン混合標準液を測定し, それぞれのピークの分離状況を比較した。Fig.1に移動相の条件1: A1-A2を用いた場合のMRMクロマトグラムを示す。A1およびA2の比率を変動させてC₆₀とC₇₀の分離状況を比較した結果, A1/A2=45%/55%の条件では, C₆₀とC₇₀のピークが完全に重なり, 両者のピークの分離は得られなかったが, A1/A2=36%/64%ではC₆₀のピークにC₇₀のショルダーピークが観察されるようになり, さらにA1/A2=27%/73%ではC₆₀とC₇₀のピークは完全に分離した。

Fig.2に移動相の条件2: B1-B2を用いた場合のMRMク

ロマトグラムを示す。B1 / B2の比率を変動させてC₆₀とC₇₀の分離状況を比較した結果、B1 / B2=70% / 30%の条件ではC₆₀のピークにC₇₀のショルダーピークが観察された。一方、B1 / B2=60% / 40%の条件ではC₆₀とC₇₀のピークは完全に分離し、B1 / B2=50% / 50%の条件ではC₆₀とC₇₀のピークの間隔がさらに広がった。

C₆₀とC₇₀のピークは条件1に比べ、条件2の移動相により良好なピーク分離が観察された。また、条件1に比べ条件2においてC₇₀のピーク形状がシャープであり、検出感度も良好であった。以上の結果から、移動相としてトルエンとアセトニトリルを用いることとした。

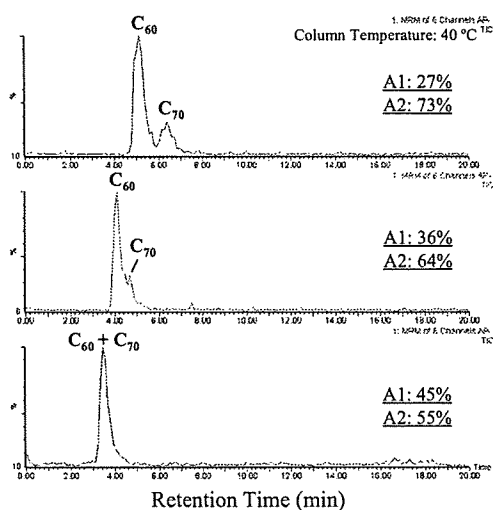


Fig. 1 Comparison of separation of fullerenes C₆₀ and C₇₀ by Atlantis dC18 separation column, A1: 2-Propanol/Toluene (1:9 v/v); A2: 2-Propanol, flow rate: 0.2mL/min, injection volume: 5 μ L

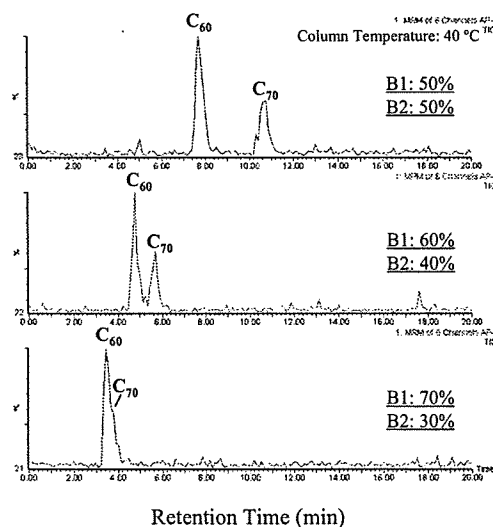


Fig. 2 Comparison of separation of fullerenes C₆₀ and C₇₀ by Atlantis dC18 separation column, B1: Toluene; B2: Acetonitrile, flow rate: 0.2mL/min, injection volume: 5 μ L

3.2 分離カラムの検討

分離カラムの検討を行った。Atlantis dC18カラムおよびC30系逆相カラムのDevelosil RPFULLERENEカラムを用いてそれぞれ100μg/LのC₆₀とC₇₀のトルエン混合標準液を測定し、ピーク分離状況を比較した。Develosil RPFULLERENEカラムで、移動相がB1 / B2=50% / 50%ではC₆₀とC₇₀のピークは20分以内に溶出せず、B1 / B2=60% / 40%ではC₆₀のみ20分以内に溶出した（データ示さず）。一方、B1 / B2=70% / 30%、カラムオープン温度が40°Cの条件において、20分以内に両ピークとも溶出され、シャープなピークが観察された。また、C₆₀とC₇₀のピークはそれぞれのピークトップの間隔が3分程度というように十分な分離能が確認され、検出感度も良好であった (Fig. 3)。一方、同じ条件において、Atlantis dC18カラムではC₆₀とC₇₀のピーク分離は不十分でありピーク形状も良くなかった (Fig.2)。さらに、Develosil RPFULLERENEカラムにおいてカラムオープン温度を30°Cにして分離状況を比較したところ、40°Cに比べC₆₀とC₇₀のピークはそれぞれのピークトップの間隔が4分程度というようにより良好に分離することが確認された (Fig.3)。以上の結果から、LC-MS/MSの諸条件を下記にまとめた。

装置 : Waters Alliance 2695,

Waters Micromass Quattro micro API

分離カラム : Develosil RPFULLERENE (5 μm, 4.6 ×

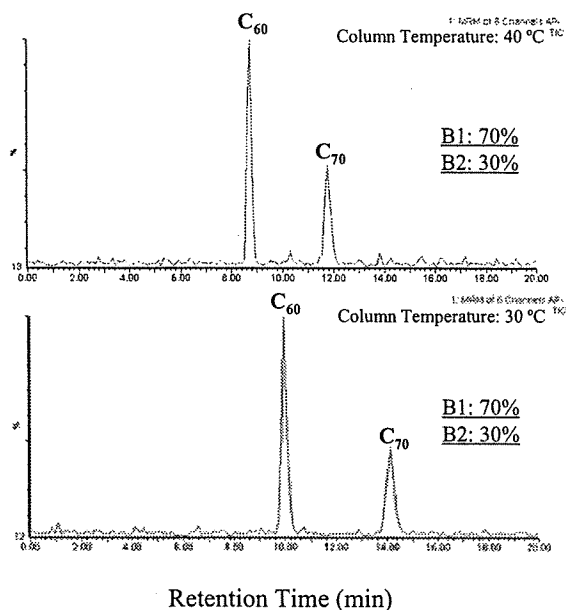


Fig. 3 Comparison of separation of fullerenes C₆₀ and C₇₀ by Develosil RPFULLERENE separation column, B1: Toluene; B2: Acetonitrile, flow rate: 1mL/min, injection volume: 20 μ L

250 mm)

移動相：トルエン/アセトニトリル=70%/30%

アイソクラティック法

流速：1mL/min

カラムオープン温度：30℃

試料注入量：20μL

イオン化法：APCIネガティブイオンモード

この条件では定量下限値は10μg/Lであった。すなわち組織重量に換算すると1.1μg/g wet wt.であった。

3.3 生物試料を対象としたフラーレンの抽出方法の検討

実験動物の臓器からのフラーレンの抽出方法を確立するため、実験動物の臓器組織を用いたフラーレンの添加回収試験を行った。検討には日本SLC(株)から購入したSlc:Wistar(SPF)ラット雄6週齢から得た肝臓、腎臓、脾臓、肺、脳、および血液を用いた。血液および全ての臓器においてC₆₀の回収率は100%前後(平均値±標準偏差:102.7±3.9%)と良好な結果が得られた(Fig.4)。また、MRMクロマトグラムにおいても、全ての臓器から抽出した試料において良好なピーク形状が得られ、また、妨害ピークや干渉等は認められなかった。C₇₀の回収率についても100%前後と良好な結果(平均値±標準偏差:98.6±4.5%)が得られたことから、C₇₀をサロゲートとして用いることが妥当であることが示された。C₇₀の回収率を用いC₆₀の回収率補正を行った結果、補正前(102.7±3.9%)と補正後(104.4±6.6%)でC₆₀の回収率はほぼ同程度であった。以上の結果より、曝露評価のために本研究で示したトルエンによる振とう抽出法によって組織中のC₆₀の分析を行うことができ、生物試料を対象と

する際にC₇₀により抽出効率の補正を行うことでより正確な分析が可能であることが示された。

4. おわりに

フラーレンのヒトにおける健康影響評価を最終目標に、LC-MS/MSによりC₇₀を抽出操作の補正として用いるC₆₀の測定法、さらには生物試料を対象としたフラーレンの抽出方法を検討した。本報で示した方法により、生物試料を対象としたフラーレンの分析が可能となり、曝露評価を実施する有効な方法であると言える。

参考文献

- 1) Nel, A., Xia, T., Mädler, L., Li, N.: *Science*, 3, 622-627 (2006).
- 2) Colvin, V. L.: *Nat. Biotechnol.*, 21, 10, 1166-1170 (2003).
- 3) Moore, M.N.: *Environ. Int.*, 32, 967-976 (2006)
- 4) Kroto, H.W., Heath, J.R., O' Brien, S.C., Curl, R.F., SamLley, R.E.: *Nature*, 318, 14, 162-163 (1985)
- 5) Dugan, L. L., Turetsky, D. M., Du, C., Lobner, D., Wheeler, M., AlmLi, C. R., Shen, C. K. F., Luh, T. Y., Choi, D. W., Lin, T. S.: *Proc. Natl. Acad. Sci. USA*, 94, 9434-9439 (1997)
- 6) Tokuyama, H., Yamago, S., Nakamura, E.: *J. Am. Chem. Soc.*, 115, 7918-7919 (1993)
- 7) Friedman, S. H., DeCamp, D. L., Sijbesma, R. P., Srdanov, G., Wudl, F., Kenyon, G. L.: *J. Am. Chem. Soc.*, 115, 6506-6509 (1993)
- 8) Sayes, C. M., Gobin, A. M., Ausman, K. D., Mendez, J., West, J. L., Colvin, V. L.: *Biomaterials*, 26, 7587-7595 (2005)
- 9) Bosi, S., Da Ros, T., Spalluto, G., Prato, M.: *Eur. J. Med. Chem.*, 38, 11-12, 913-923 (2003)
- 10) Lovorn, S.B., Klaper, R.: *Environ. Toxicol. Chem.*, 25, 4, 1132-1137 (2006)
- 11) Yamago, S., Tokuyama, H., Nakamura, E., Kikuchi, K., Kananishi, S., Sueki, K., Nakahara, H., Enomoto, S., Ambe, F.: *Chem. Biol.*, 2, 385-389 (1995)
- 12) Moussa, F., Pressac, M., Genin, E., Roux, S., Trivin, F., Rassat, A., Célin, R., Szwarc, H.: *J. Chromatogr. B*, 696, 153-159 (1997)
- 13) Xia, X. R., Monteiro-Riviere, N. A., Riviere, J. E.: *J. Chromatogr. A*, 1129, 216-222 (2006)
- 14) Moussa, F., Pressac, M., Genin, E., Roux, S., Trivin, F., Rassat, A., Célin, R., Szwarc, H.: *J. Chromatogr. B*, 696, 153-159 (1997)

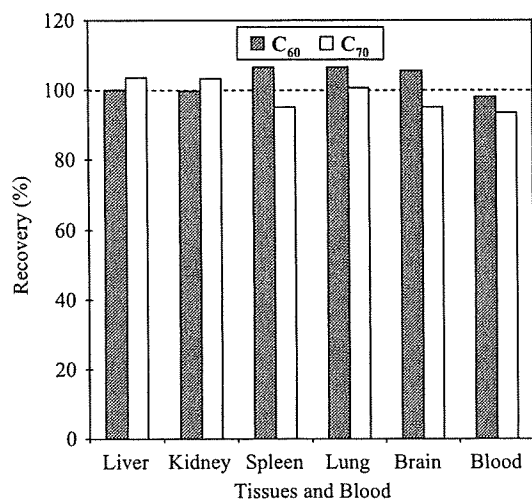


Fig. 4 Comparison of recovery of fullerenes C₆₀ and C₇₀ from tissues and blood of Slc:Wistar(SPF) rat.

Letter

Serum level of expressed in renal carcinoma (ERC)/ mesothelin in rats with mesothelial proliferative lesions induced by multi-wall carbon nanotube (MWCNT)

Yoshimitsu Sakamoto¹, Dai Nakae^{1,2}, Yoshiaki Hagiwara^{3,4}, Kanako Satoh¹,
Norio Ohashi¹, Katsumi Fukamachi⁵, Hiroyuki Tsuda⁵, Akihiko Hirose⁶, Tetsuji Nishimura⁷,
Okio Hino³ and Akio Ogata¹

¹Department of Environmental Health and Toxicology, Tokyo Metropolitan Institute of Public Health, 3-24-1
Hyakunin'cho, Shinjuku-ku, Tokyo 169-0073, Japan

²Tokyo University of Agriculture, 1-1-1 Sakuragaoka, Setagaya-ku, Tokyo, 156-8502, Japan

³Department of Pathology and Oncology, Juntendo University School of Medicine, 2-1-1 Hongo, Bunkyo-ku, Tokyo
113-8421, Japan

⁴Immuno-Biological Laboratory Co., Ltd., 1091-1 Naka, Fujioka, Gunma 375-0005, Japan

⁵Department of Molecular Toxicology, Nagoya City University, 1 Kawasumi, Mizuho-cho, Mizuho-ku, Nagoya,
Aichi 467-8601, Japan

⁶Divisions of Risk Assessment, Biological Safety Research Center and ⁷Environmental Chemistry, National Institute of
Health Sciences, 1-18-1 Kamiyoga, Setagaya-ku, Tokyo 158-8501, Japan

(Received November 5, 2009; Accepted December 30, 2009)

ABSTRACT — Expressed in renal carcinoma (ERC)/mesothelin is a good biomarker for human mesothelioma and has been investigated for its mechanistic rationale during the mesothelioma development. Studies are thus ongoing in our laboratories to assess expression of ERC/mesothelin in sera and normal/proliferative/neoplastic mesothelial tissues of animals untreated or given potentially mesothelioma-inducible xenobiotics, by an enzyme-linked immunosorbent assay (ELISA) for N- and C-(terminal fragments of) ERC/mesothelin and immunohistochemistry for C-ERC/mesothelin. In the present paper, we intend to communicate our preliminary data, because this is the first report to show how and from what stage the ERC/mesothelin expression changes during the chemical induction of mesothelial proliferative/neoplastic lesions. Serum N-ERC/mesothelin levels were 51.4 ± 5.6 ng/ml in control male Fischer 344 rats, increased to 83.6 ± 11.2 ng/ml in rats given a single intrascrotal administration of 1 mg/kg body weight of multi-wall carbon nanotube (MWCNT) and bearing mesothelial hyperplasia 52 weeks thereafter, and further elevated to 180 ± 77 ng/ml in rats similarly treated and becoming moribund 40 weeks thereafter, or killed as scheduled at the end of week 52, bearing mesothelioma. While C-ERC/mesothelin was expressed in normal and hyperplastic mesothelia, the protein was detected only in epithelioid mesothelioma cells at the most superficial layer. It is thus suggested that ERC/mesothelin can be used as a biomarker of mesothelial proliferative lesions also in animals, and that the increase of levels may start from the early stage and be enhanced by the progression of the mesothelioma development.

Key words: Serum mesothelin, Rat, MWCNT, Mesothelial proliferative lesions

INTRODUCTION

Mesothelioma is a highly aggressive malignant tumor and developed in people previously exposed to asbestos, after a long latency period of 30-40 years. It is desired to establish a biomarker that can identify potential patients

with early stage tumors or even as yet without tumors among the high-risk population.

Expressed in renal carcinoma (ERC)/mesothelin is a product of the *Erc* gene discovered in renal carcinomas of the Eker rats (Hino *et al.*, 1995) and confirmed as a homolog of the human *mesothelin/megakaryocyte poten-*

Correspondence: Yoshimitsu Sakamoto (E-mail: Yoshimitsu_Sakamoto@member.metro.tokyo.jp)

ciating factor gene (Hino, 2004; Yamashita *et al.*, 2000). A 71-kDa glycosylphosphatidylinositol anchor-type membranous protein is produced and physiologically cleaved by a furin-like protease to yield a membrane-binding 40-kDa C-terminal (C-ERC/mesothelin) and a secreting 31-kDa N-terminal (N-ERC/mesothelin) fragments (Chang and Pastan, 1996; Maeda and Hino, 2006; Yamaguchi, *et al.*, 1994). ERC/mesothelin is a useful marker for human mesothelioma cases (Hino *et al.*, 2007; Maeda and Hino, 2006) and its specific enzyme-linked immunosorbent assay (ELISA) system has been developed (Hagiwara *et al.*, 2008; Nakaishi *et al.*, 2007) for the clinical use (Maeda and Hino, 2006; Shiomi, *et al.*, 2006, 2008; Tajima *et al.*, 2008). The most important question is as to whether ERC/mesothelin can be efficient also in the early phase of the mesothelioma development, and studies are ongoing in our laboratories to assess ERC/mesothelin levels in animals untreated or given potentially mesothelioma-inducible xenobiotics.

We preliminarily assessed ERC/mesothelin levels using the samples of our previous study demonstrating the induction of mesothelial proliferative lesions in male Fisher 344 rats given multi-wall carbon nanotube (MWCNT) (Sakamoto *et al.*, 2009). In the present paper, we intend to communicate this preliminary data, despite its very limited sample numbers, because this is the first report to show how and from what stage the ERC/mesothelin expression changes during the chemical induction of mesothelial proliferative/neoplastic lesions.

MATERIALS AND METHODS

Ethical consideration of the experiments

An experimental protocol was approved by the Experiments Regulation/Animal Experiment Committees of the Tokyo Metropolitan Institute of Public Health for its scientific and ethical appropriateness, including concern for animal welfare, with strict obedience to domestically and internationally applicable declarations, laws, guidelines and rules.

Samples

Male Fisher 344 rats were purchased at their age of 4 weeks old from Charles River Laboratories Japan Inc. (Kanagawa, Japan) and maintained in our animal room (24–25°C, 50–60% relative humidity, 10 times/hr air ventilation and 12-hr light/dark cycle) until use.

Normal rat samples

Serum samples were obtained from 3, 1 and 2 untreated rats at their ages of 11, 42 and 81 weeks old, respectively.

Vehicle/MWCNT-treated rat samples

As detailed elsewhere (Sakamoto *et al.*, 2009), rats were given a single intrascrotal administration of 1 ml/kg body weight of vehicle (2% carboxymethylcellulose) or 1 mg/kg body weight of MWCNT at the age of 12 weeks old and left untreated for up to 52 weeks. In the present study, 9 samples were used: 3 from vehicle-treated rats killed as scheduled at the end of week 52, without any mesothelial changes; 3 from MWCNT-treated rats similarly killed, with mesothelial hyperplasias but without mesotheliomas; and 3 from other MWCNT-treated animals, 1 killed as moribund at week 40 and 2 killed as scheduled at the end of week 52, with early and advanced stages mesotheliomas and hemorrhagic ascites. Serum samples and in the last case an ascites sample were obtained at the time of the autopsy, and 10% neutrally buffered formalin-fixed, paraffin-embedded, mesothelial tissue samples were routinely prepared.

ERC/mesothelin ELISA assay

Serum and ascites ERC/mesothelin levels were analyzed using rat N- and C-ERC/mesothelin assay kits (Immuno-Biological Laboratories [IBL] Co., Ltd., Gunma, Japan) adapting from the method of Hagiwara *et al.* (2008), the detection limit being 0.1 ng/ml. A 6- μ l aliquot was diluted with 234 μ l of phosphate-buffered saline containing 1% bovine serum albumin and 0.05% Tween 20. Assays were conducted according to the manufacturer's instruction to measure an optical density at 450 nm. Each sample was assessed in duplicate.

Histology and C-ERC/mesothelin immunohistochemistry

Two serial, 4- μ m-thick sections were prepared and deparaffinized. One was processed through a routine hematoxylin and eosin (HE) staining procedure and histologically examined. The other was heated in 10 mM citrate buffer, pH 6.0, treated with 3% hydrogen peroxide, incubated with a primary anti-rat C-ERC/mesothelin antibody (IBL) overnight at 4°C, washed with tris-buffered saline, and re-incubated using an Envision system (DAKO Japan Company, Limited, Tokyo, Japan). Signals were visualized by 3,3'-diaminobenzidine, and the sections were counter-stained with hematoxylin.

Statistical analysis

Statistical significance of intergroup difference for the N-ERC/mesothelin level was assessed using Student's *t*-test, and *p*-values less than 0.05 were considered significant.

Serum ERC/mesothelin level in rats with mesothelial proliferative lesions

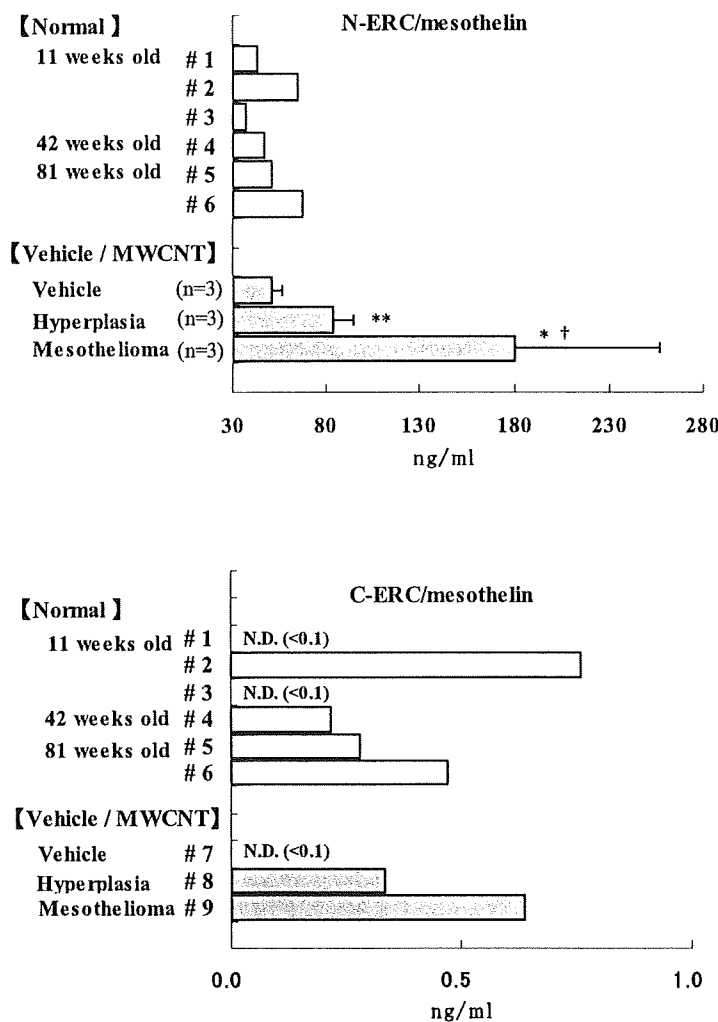


Fig. 1. Serum levels of A, N-ERC/mesothelin and B, C-ERC/mesothelin. Each data is a mean of duplicate assays. #1- #6 in Fig. A and #1- #9 in Fig. B show sample numbers. "N.D.", not detectable, indicates that the data was below the detection limit of 0.10 ng/ml. Values of N-ERC/mesothelin of samples from vehicle, hyperplasia and mesothelioma groups in Fig. B represent the means \pm S.D. (n = 3). Statistical significant difference by Student's t-test: * $P < 0.05$, ** $P < 0.01$ as compared from the vehicle group and † $P < 0.05$ as compared from the hyperplastic group.

RESULTS AND DISCUSSION

Serum N-ERC/mesothelin levels of the normal rats were 43.4, 65.1 and 37.3 ng/ml, 47.1 ng/ml and 51.1 and 67.5 ng/ml; while those of C-ERC/mesothelin were < 0.1, 0.8 and < 0.1 ng/ml, 0.2 ng/ml and 0.3 and 0.5 ng/ml; for 11, 42 and 81 weeks of their ages, respectively (Fig. 1). These were respectively within the same range, and the

N-ERC/mesothelin levels were substantially higher than the C-ERC/mesothelin levels. No apparent age-dependent changes were obtained for either fragment.

Serum N-(n = 3) and C-(n = 3) ERC/mesothelin levels of the vehicle-treated rat was 51.4 ± 5.6 ng/ml and < 0.1 ng/ml, respectively, within the normal ranges, whereas serum N-ERC/mesothelin levels of MWCNT-treated rats were increased by the induction of mesothelial hyperplasia-

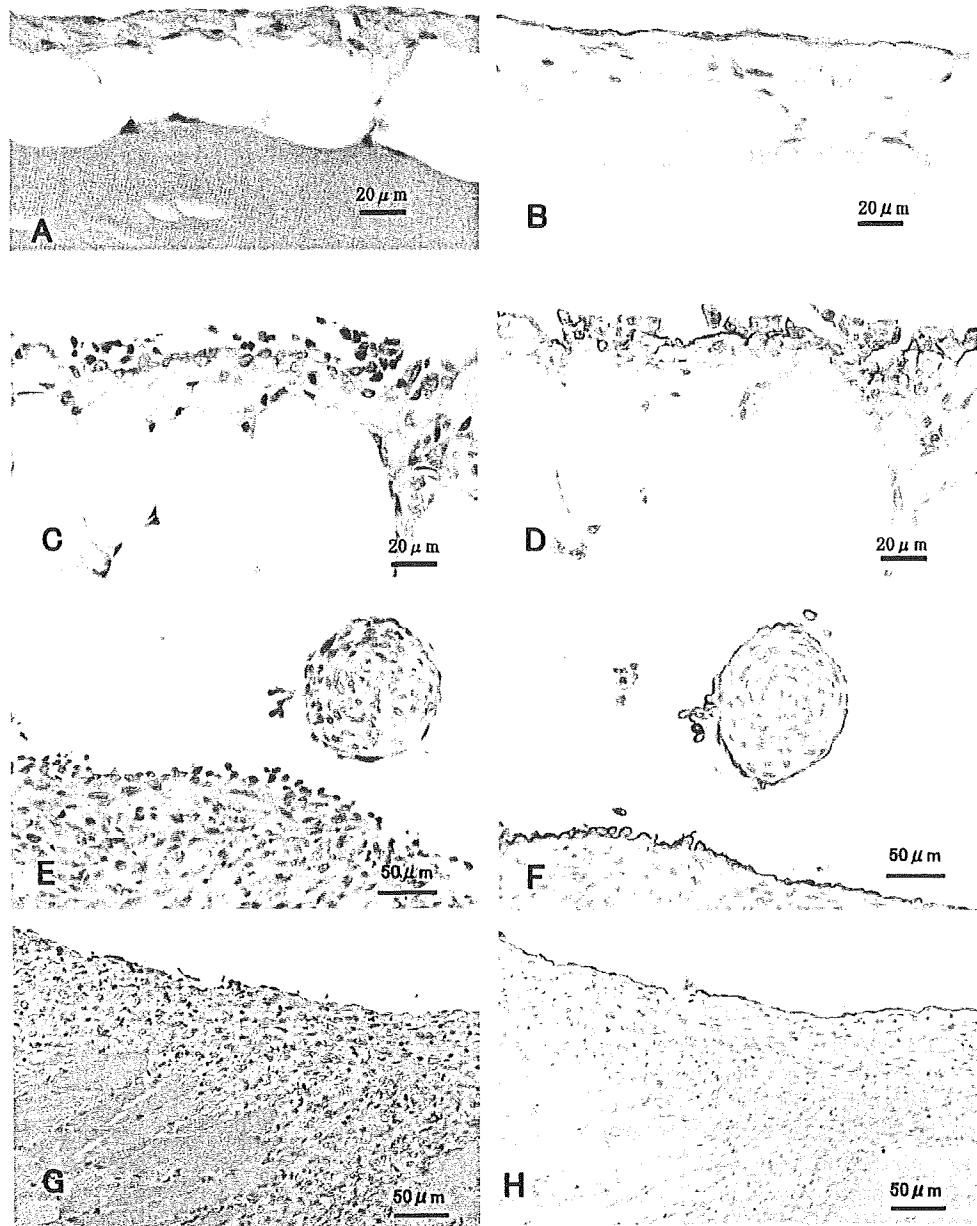


Fig. 2. Representative histology and C-ERC/mesothelin immunohistochemistry. A, intact mesothelium in the parietal peritoneum of the vehicle-treated rat, HE; B, A's serial section, C-ERC/mesothelin; C, a mesothelial hyperplasia in the retroperitoneal fat tissue of the MWCNT-treated rat, HE; D, C's serial section, C-ERC/mesothelin; E, an early-stage epithelioid/polypoid type mesothelioma in retroperitoneal fat tissue of the other MWCNT-treated rat, HE; F, E's serial section, C-ERC/mesothelin; G, an advanced-stage mostly-sarcomatoid/invasive-nodular type mesothelioma in the diaphragm of the MWCNT-treated rat (the same animal as E/F), HE; H, G's serial section, C-ERC/mesothelin. Bars with their lengths are inserted to indicate magnifications.

Serum ERC/mesothelin level in rats with mesothelial proliferative lesions

sia (83.6 ± 11.2 ng/ml) and further by that of mesothelioma (179 ± 77 ng/ml; $3,004 \pm 665$ ng/ml in ascites) (Fig. 1). Serum N-ERC/mesothelin levels in experimental animals have only been assessed in Eker and Wistar rats and nude mice, untreated or transplanted with a rat mesothelioma cell line, MetEt-40 (Hagiwara *et al.*, 2008; Nakaishi *et al.*, 2007). The present data for the first time demonstrates that serum N-ERC/mesothelin level was increased already at the stage of preneoplastic, mesothelial hyperplasia and further increased by the chemical induction of mesothelioma. This may be in line with the recent findings that elevated serum mesothelin is detected before the development of grossly visible carcinoma lesions in a rat pancreatic carcinoma models (Fukamachi *et al.*, 2009). In human mesothelioma, it has been reported that N-ERC/mesothelin level increased with the stage went up of epithelioid type mesothelioma in human case (Shiomi *et al.*, 2008). It is not known, however, how N-ERC/mesothelin levels change in the stage of preneoplasia at this moment. Large-scaled, detailed investigations using the MWCNT-mesothelioma model are ongoing in our laboratories.

Serum C-ERC/mesothelin levels of MWCNT-treated rats were 0.4 and 0.6 ng/ml, within the normal/vehicle range (Fig. 1B). This is in accordance with the previous finding in nude mice transplanted with MetEt-40 (Hagiwara *et al.*, 2008), and can be attributed to the membrane-binding property of C-ERC/mesothelin (Maeda and Hino, 2006). Ascites level of C-ERC/mesothelin in the mesothelioma case was slightly increased to 10.9 ng/ml (Fig. 1B). This is speculated to result from a release of C-ERC/mesothelin by phosphatidylinositol-specific phospholipase C (Chang and Pastan, 1996) or a contamination of desquamated mesothelioma cells.

Immunohistochemical C-ERC/mesothelin signals were constantly detected in cell membranes. C-ERC/mesothelin was detected in intact (Figs. 2A and B) and hyperplastic (Figs. 2C and D) mesothelia. Taken the ELISA data together, it might be possible that the ERC/mesothelin level starts increased from the preneoplastic stage.

C-ERC/mesothelin was found only in epithelioid (mesothelioid) tumor cells present at the most superficial layer of early-stage, epithelioid/polypoid (Figs. 2E and F) and advanced-stage, mostly-sarcomatoid/invasive-nodular (Figs. 2G and H) types of mesotheliomas. In humans, epithelioid types, but not sarcomatoid types or sarcomatoid components of biphasic (mixed) types, immunohistochemically express C-ERC/mesothelin (Chang and Pastan, 1996; Shiomi *et al.*, 2008; Ordóñez, 2003). Accordingly, serum N-ERC/mesothelin levels were only slightly increased or often unchanged in sarcomatoid and biphasic types, in contrast to the epithe-

lioid type (Hassan *et al.*, 2006; Shiomi *et al.*, 2008). The present findings suggest that the increase of ERC/mesothelin levels in mesotheliomas may be a universal event for all types and stages, and that C-terminal fragments may become unproduced or changed its tertiary structure and/or epitope construction by the neoplastic conversion.

In conclusion, the present data suggests that ERC/mesothelin can be used as a biomarker of mesothelial proliferative lesions also in animals, and that its increase of its levels may start from the early stage and be enhanced by the progression of the mesothelioma development.

ACKNOWLEDGMENTS

This work was supported in part by a research budget of the Tokyo Metropolitan Government, Japan, and Grants-in-Aid for Scientific Research from the Ministry of Health, Labour and Welfare of Japan, from the Japan Society for the Promotion of Science, and from the Ministry of Education, Culture, Sports, Science and Technology of Japan. This study was also partially supported by a consignment expense for Molecular Imaging Program on "Research Base for PET Diagnosis" from the Ministry of Education, Culture, Sports, Science and Technology of Japan.

REFERENCES

- Chang, K. and Pastan, I. (1996): Molecular cloning of mesothelin, a differentiation antigen present on mesothelium, mesotheliomas, and ovarian cancers. *PNAS USA*, **93**, 136-140.
- Fukamachi, K., Tanaka, H., Hagiwara, Y., Ohara, H., Joh, T., Iigo, M., Alexander, D.B., Xu, J., Long, N., Takigahira, M., Yanagihara, K., Hino, O., Saito, I. and Tsuda, H. (2009): An animal model of preclinical diagnosis of pancreatic ductal carcinomas. *Biochem. Biophys. Res. Commun.*, **390**, 636-641.
- Hagiwara, Y., Hamada, Y., Kuwahara, M., Maeda, M., Segawa, T., Ishikawa, K. and Hino, O. (2008): Establishment of a novel specific ELISA system for rat N- and C-ERC/mesothelin. *Rat ERC/mesothelin in the body fluids of mice bearing mesothelioma. Cancer Sci.*, **99**, 666-670.
- Hassan, R., Remaley, A.T., Sampson, M.L., Zhang, J., Cox, D.D., Pingpank, J., Alexander, R., Willingham, M., Pastan, I. and Onda, M. (2006): Detection and quantitation of serum mesothelin, a tumor marker for patients with mesothelioma and ovarian cancer. *Clin. Cancer Res.*, **12**, 447-453.
- Hino, O., Kobayashi, E., Nishizawa, M., Kubo, Y., Kobayashi, T., Hirayama, Y., Takai, S., Kikuchi, Y., Tsuchiya, H., Orimoto, K., Kajino, K., Takahata, T. and Hitani, H. (1995): Renal carcinogenesis in the Eker rat. *J. Cancer Res. Clin. Oncol.*, **121**, 602-605.
- Hino, O. (2004): Multistep renal carcinogenesis in the Eker (*Tsc2* gene mutant) rat model. *Curr. Mol. Med.*, **4**, 807-811.
- Hino, O., Shiomi, K. and Maeda, M. (2007): Diagnostic biomarker of asbestos-related mesothelioma: example of translational research. *Cancer Sci.*, **98**, 1147-1151.

- Maeda, M. and Hino, O. (2006): Molecular tumor markers for asbestos-related mesothelioma: serum diagnostic markers. *Pathol. Int.*, **56**, 649-654.
- Ordóñez, N.G. (2003): Value of mesothelin immunostaining in the diagnosis of mesothelioma. *Mod. Pathol.*, **16**, 192-197.
- Nakaishi, M., Kajino, K., Ikesue, M., Hagiwara, Y., Kuwahara, M., Mitani, H., Horikoshi-Sakuraba, Y., Segawa, T., Kon, S., Maeda, M., Wang, T., Abe, M., Yokoyama, M. and Hino, O. (2007): Establishment of the enzyme-linked immunosorbent assay system to detect the amino terminal secretory form of rat Erc/Mesothelin. *Cancer Sci.*, **98**, 659-664.
- Sakamoto, Y., Nakae, D., Fukumori, N., Tayama, K., Maekawa, A., Imai, K., Hirose, A., Nishimura, T., Ohashi, N. and Ogata, A. (2009): Induction of mesothelioma by a single intrascrotal administration of multi-wall carbon nanotube in intact male Fischer 344 rats. *J. Toxicol. Sci.*, **34**, 65-76.
- Shiomi, K., Miyamoto, H., Segawa, T., Hagiwara, Y., Ota, A., Maeda, M., Takahashi, K., Masuda, K., Sakao, Y. and Hino, O. (2006): Novel ELISA system for detection of N-ERC/mesothelin in the sera of mesothelioma patients. *Cancer Sci.*, **97**, 928-932.
- Shiomi, K., Hagiwara, Y., Sonoue, K., Segawa, T., Miyashita, K., Maeda, M., Izumi, H., Masuda, K., Hirabayashi, M., Moroboshi, T., Yoshiyama, T., Ishida, A., Natori, Y., Inoue, A., Kobayashi, M., Sakao, Y., Miyamoto, H., Takahashi, K. and Hino, O. (2008): Sensitive and specific new enzyme-linked immunosorbent assay for N-ERC/mesothelin increases its potential as a useful serum tumor marker for mesothelioma. *Clin. Cancer Res.*, **14**, 1431-1437.
- Tajima, K., Hirama, M., Shiomi, K., Ishiwata, T., Yoshioka, M., Iwase, A., Iwakami, S., Yamazaki, M., Toba, M., Tobino, K., Sugano, K., Ichikawa, M., Hagiwara, Y., Takahashi, K. and Hino, O. (2008): ERC/mesothelin as a marker for chemotherapeutic response in patients with mesothelioma. *Anticancer Res.*, **28**, 3933-3936.
- Yamaguchi, N., Hattori, K., Oheda, M., Kojima, T., Imai, N. and Ochi, N. (1994): A novel cytokine exhibiting megakaryocyte potentiating activity from a human pancreatic tumor-cell line HPC-Y5. *J. Biol. Chem.*, **269**, 805-808.
- Yamashita, Y., Yokoyama, M., Kobayashi, E., Takai, S. and Hino, O. (2000): Mapping and determination of the cDNA sequence of the *Erc* gene preferentially expressed in renal cell carcinoma in the *Tsc2* gene mutant (Eker) rat model. *Biochem. Biophys. Res. Commun.*, **275**, 134-140.

Involvement of macrophage inflammatory protein 1 α (MIP1 α) in promotion of rat lung and mammary carcinogenic activity of nanoscale titanium dioxide particles administered by intra-pulmonary spraying

Jieyou Xu¹, Mitsuru Futakuchi¹, Masaaki Iigo¹, Katsumi Fukamachi¹, David B. Alexander¹, Hideo Shimizu², Yuto Sakai^{1,3}, Seiko Tamano⁴, Fumio Furukawa⁴, Tadashi Uchino⁵, Hiroshi Tokunaga⁶, Tetsuji Nishimura⁵, Akihiko Hirose⁵, Jun Kanno⁵ and Hiroyuki Tsuda^{1,*}

¹Department of Molecular Toxicology and ²Core Laboratory, Nagoya City University Graduate School of Medical Sciences, 1-Kawasumi, Mizuho-cho, Mizuho-ku, Nagoya 467-8601, Japan, ³Department of Drug Metabolism and Disposition, Graduate School of Pharmaceutical Sciences, 3-1, Tanabe-Dohri, Mizuho-ku, Nagoya 467-8603, Japan, ⁴DIMS Institute of Medical Science, Inc., 64 Goura, Nishiazai, Azai-cho, Ichinomiya 491-0113, Japan, ⁵National Institute of Health Sciences, 1-18-1 Kamiyoga, Setagaya-ku, Tokyo 158-8501, Japan and ⁶Pharmaceuticals and Medical Devices Agency, 2-3-3, Kasumigaseki, Chiyoda-ku, Tokyo 100-0013, Japan

*To whom correspondence should be addressed. Tel: +81 52 853 8991; Fax: +81 52 853 8996; Email: htsuda@med.nagoya-cu.ac.jp

Titanium dioxide (TiO₂) is evaluated by World Health Organization/International Agency for Research on Cancer as a Group 2B carcinogen. The present study was conducted to detect carcinogenic activity of nanoscale TiO₂ administered by a novel intrapulmonary spraying (IPS)-initiation-promotion protocol in the rat lung. Female human c-Ha-*ras* proto-oncogene transgenic rat (*Hras128*) transgenic rats were treated first with *N*-nitrosobis(2-hydroxypropyl)amine (DHPN) in the drinking water and then with TiO₂ (rutile type, mean diameter 20 nm, without coating) by IPS. TiO₂ treatment significantly increased the multiplicity of DHPN-induced alveolar cell hyperplasias and adenomas in the lung, and the multiplicity of mammary adenocarcinomas, confirming the effectiveness of the IPS-initiation-promotion protocol. TiO₂ aggregates were localized exclusively in alveolar macrophages and had a mean diameter of 107.4 nm. To investigate the underlying mechanism of its carcinogenic effects, TiO₂ was administered to wild-type rats by IPS five times over 9 days. TiO₂ treatment significantly increased 8-hydroxydeoxy guanosine level, superoxide dismutase activity and macrophage inflammatory protein 1 α (MIP1 α) expression in the lung. MIP1 α , detected in the cytoplasm of TiO₂-laden alveolar macrophages *in vivo* and in the media of rat primary alveolar macrophages treated with TiO₂ *in vitro*, enhanced proliferation of human lung cancer cells. Furthermore, MIP1 α , also detected in the sera and mammary adenocarcinomas of TiO₂-treated *Hras128* rats, enhanced proliferation of rat mammary carcinoma cells. These data indicate that secreted MIP1 α from TiO₂-laden alveolar macrophages can cause cell proliferation in the alveoli and mammary gland and suggest that TiO₂ tumor promotion is mediated by MIP1 α acting locally in the alveoli and distantly in the mammary gland after transport via the circulation.

Abbreviations: CCR1, C-C chemokine receptor type 1; DHPN, *N*-nitrosobis(2-hydroxypropyl) amine; ERK, extracellular signal-regulated kinase; GRO, growth-regulated oncogene; *Hras128* rat, human c-Ha-*ras* proto-oncogene transgenic rat; IL, interleukin; IPS, intrapulmonary spraying; MEK1, MAPK/ERK kinase1; MIP1 α , macrophage inflammatory protein 1 α ; 8-OHdG, 8-hydroxydeoxy guanosine; PBS, phosphate-buffered saline; ROS, reactive oxygen species; SD, Sprague-Dawley; SOD, superoxide dismutase; TEM, transmission electron microscopy; TiO₂, titanium dioxide.

Introduction

Inhalation of particles and fiber is well known to be strongly associated with increased lung cancer risk in the workplace (1,2). Although the size of fiber particles was reported to be closely related to risk (3), the precise role of particles and fibers in lung cancer induction has not yet been elucidated.

Titanium dioxide (TiO₂) particles of various sizes are manufactured worldwide in large quantities and are used in a wide range of applications. TiO₂ particles have long been considered to pose little risk to respiratory health because they are chemically and thermally stable. However, TiO₂ is classified as a Group 2B carcinogen, a possible carcinogen to humans, by World Health Organization/International Agency for Research on Cancer based on the findings of lung tumor induction in female rats (3,4). This overall evaluation includes nanoscale (<100 nm in diameter) and larger sized classes of TiO₂. At present, the mechanism underlying the development of rat lung tumors by inhalation of TiO₂ particles is unclear.

Inhalation of TiO₂ particles can occur both at the workplace, e.g. in manufacturing and packing sites, and also outside the workplace during their use (5–7). Exposure to airborne nanoparticles has been reported to be associated with a granulomatous inflammatory response in the lung (8). Inhalation studies of nanoparticles for cancer risk assessment is urgently needed, however, due to the high cost of long-term studies, available data is severely limited (9,10). The aim of this study is to understand the mechanism underlying rat lung carcinogenesis induced by inhalation of TiO₂ particles. We choose intrapulmonary spraying (IPS) because it does not require costly facilities, allows accurate dose control and approximates long-term inhalation studies (3,11).

We initially examined whether TiO₂ particles have carcinogenic activity in the rat lung using a novel IPS-initiation-promotion protocol (12,13). For these experiments, Sprague-Dawley (SD)-derived female human c-Ha-*ras* proto-oncogene transgenic rat (*Hras128*) transgenic rats, which are known to have the same carcinogen susceptibility phenotype in the lung as wild-type rats but are highly susceptible to mammary tumor induction (14–16), were treated with *N*-nitrosobis(2-hydroxypropyl)amine (DHPN) to initiate carcinogenesis and then treated with TiO₂ by IPS. We observed a promotion effect of TiO₂ particles in lung and mammary gland carcinogenesis.

To identify factors involved in this promotion effect, wild-type SD strain rats were treated with TiO₂ by IPS for 9 days. We found macrophage inflammatory protein 1 α (MIP1 α) was produced by TiO₂-laden alveolar macrophages in the lungs of rats treated with TiO₂. MIP1 α is a member of the CC chemokine family and is primarily associated with cell adhesion and migration of multiple myeloma cells (17). It is reported to be produced by macrophages in response to a variety of inflammatory stimuli including TiO₂ (18). In the present study, MIP1 α , detected in the medium of rat primary alveolar macrophages treated with TiO₂, enhanced proliferation of human lung cancer cells *in vitro*. MIP1 α was also detected in the sera and mammary adenocarcinomas of TiO₂-treated *Hras128* rats and enhanced proliferation of rat mammary carcinoma cells.

Materials and methods

Animals

Female transgenic rats carrying the *Hras128* and female wild-type SD rats were obtained from CLEA Japan Co., Ltd (Tokyo, Japan) (15). The animals were housed in the animal center of Nagoya City University Medical School, maintained on a 12 h light-dark cycle and received Oriental MF basal diet (Oriental Yeast Co., Tokyo, Japan) and water *ad libitum*. The research was conducted according to the Guidelines for the Care and Use of Laboratory Animals of

Nagoya City University Medical School and the experimental protocol was approved by the Institutional Animal Care and Use Committee (H17-28).

Preparation of TiO₂ and IPS

TiO₂ particles (rutile type, without coating; with a mean primary size of 20 nm) were provided by Japan Cosmetic Association, Tokyo, Japan. TiO₂ particles were suspended in saline at 250 µg/ml or 500 µg/ml. The suspension was autoclaved and then sonicated for 20 min just before use. The TiO₂ suspension was intratracheally administered to animals under isoflurane anesthesia using a Micro-sprayer (Series IA-1B Intratracheal Aerosolizer, Penn-Century, Philadelphia, PA) connected to a 1 ml syringe; the nozzle of the sprayer was inserted into the trachea through the larynx and a total of 0.5 ml suspension was sprayed into the lungs synchronizing with spontaneous respiratory inhalation (IPS).

IPS-initiation-promotion protocol

Thirty-three female *Hras128* rats aged 6 weeks were given 0.2% DHPN, (Wako Chemicals Co., Ltd Osaka, Japan) in the drinking water for 2 weeks and 9 rats were given drinking water without DHPN. Two weeks later, the rats were divided into four groups, DHPN alone (Group 1), DHPN followed by 250 µg/ml TiO₂ (Group 2), DHPN followed by 500 µg/ml TiO₂ (Group 3) and 500 µg/ml TiO₂ without DHPN (Group 4). The TiO₂ particle preparations were administered by IPS once every 2 weeks from the end of week 4 to week 16 (a total of seven times). The total amount of TiO₂ administered to Groups 1, 2, 3 and 4 were 0, 0.875, 1.75 and 1.75 mg per rat, respectively. Three days after the last treatment, animals were killed and the organs (brain, lung, liver, spleen, kidney, mammary gland, ovaries, uterus and neck lymph nodes) were excised and divided into two pieces; one piece was immediately frozen at -80°C and used for quantitative measurement of elemental titanium, and the other piece was fixed in 4% paraformaldehyde solution in phosphate-buffered saline (PBS) buffer adjusted to pH 7.3 and processed for light microscopic examination and transmission electron microscopy (TEM); the left lungs and inguinal mammary glands were used for elemental titanium analysis and the right lungs and inguinal mammary glands were used for microscopic examination.

IPS 9 day protocol

Twenty female SD rats (wild-type counterpart of *Hras128*) aged 10 weeks were treated by IPS with 0.5 ml suspension of 500 µg/ml TiO₂ particles in saline five times over a 9 day period (Figure 2A). The total amount of TiO₂ administered was 1.25 mg per rat. Six hours after the last dose, animals were killed and the lungs and inguinal mammary glands were excised. Fatty tissue surrounding the mammary gland was removed as much as possible. The left lungs and inguinal mammary glands were used for biochemical analysis, and the right lungs were fixed in 4% paraformaldehyde solution in PBS adjusted at pH 7.3 and processed for histopathological examination and immunohistochemistry.

Light microscopic and TEM observation of TiO₂ particles in the lung

Paraffin blocks were deparaffinized and embedded in epon resin and processed for TiO₂ particle observation and titanium element analysis, using a JEM-1010 transmission electron microscope (JEOL Co. Ltd, Tokyo, Japan) equipped with an X-ray microanalyzer (EDAX, Tokyo, Japan). Size analysis of TiO₂ particles was performed using TEM photos by an image analyzer system, (IPAP, Sumika Technos Corporation, Osaka, Japan). A total of 452 particles from alveolar macrophages from rats in Group 3 (DHPN followed by 500 µg/ml TiO₂) of the IPS-initiation-promotion study and a total of 2571 particles from alveolar macrophages from rats in the IPS 9 day study were measured.

Biochemical element analysis of titanium

For the detection of elemental titanium, frozen tissue samples of 50–100 mg were digested with 5 ml concentrated HNO₃ for 22 min in a microwave oven. Titanium in the digested solutions was determined by inductively coupled plasma-mass spectrometry (HP-4500, Hewlett-Packard Co., Houston, TX) under the following conditions: RF power, 1450 W; RF refraction current, 5 W; Plasma gas current, 15 l/min; Carrier gas current, 0.91 l/min; Peri pump, 0.2 r.p.s.; Monitoring mass-*m/z* 48 (Ti); Integrating interval, 0.1 s; Sampling period 0.31 s.

Analysis of superoxide dismutase activity, 8-hydroxydeoxy guanosine and cytokine levels

For the analysis of superoxide dismutase (SOD) activity, 8-hydroxydeoxy guanosine (8-OHdG) and cytokine levels, animals exposed to TiO₂ particles for 9 days were used. For 8-OHdG levels, genomic DNA was isolated from the left lung and inguinal mammary gland with a DNA Extractor WB Kit (Wako Chemicals Co. Ltd). 8-OHdG levels were determined with an 8-OHdG ELISA Check Kit (Japan Institute for the Control of Aging, Shizuoka, Japan) and by a custom service (OHG Institute Co., Ltd, Fukuoka, Japan). For the analysis of SOD activity and inflammation-related cytokines, tissue from the left lung and inguinal mammary glands was excised and rinsed with cold PBS three times

and homogenized in 1 ml of T-PER, Tissue Protein Extraction Reagent (Pierce, Rockford, IL), containing 1% (vol/vol) proteinase inhibitor cocktail (Sigma-Aldrich, St Louis, MO). The homogenates were clarified by centrifugation at 10 000g for 5 min at 4°C. Protein content was measured using a BCA™ Protein Assay Kit (Pierce). SOD activity was determined using an SOD Assay Kit (Cayman Chemical Co., Ann Arbor, MI). The levels of interleukin (IL)-1α, IL-1β, IL-6, granulocyte-macrophage colony-stimulating factor, granulocyte colony-stimulating factor, tumor necrosis factor α, interferon γ, IL-18, monocyte chemoattractant protein 1 and MIP1α, growth-regulated oncogene (GRO) and vascular endothelial growth factor were measured by Multiplex Suspension array (GeneticLab Co., Ltd, Sapporo, Japan).

Immunohistochemistry

CD68 and MIP1α were detected using anti-rat CD68 (BMA Biomedicals, Augst, Switzerland) and anti-rat MIP1α polyclonal antibodies (BioVision, Lyon, France). Both antibodies were diluted 1:100 in blocking solution and applied to slides, and the slides were incubated at 4°C overnight. The slides were then incubated for 1 h with biotinylated species-specific secondary antibodies diluted 1:500 (Vector Laboratories, Burlingame, CA) and visualized using avidin-conjugated alkaline phosphatase complex (ABC kit, Vector Laboratories) and Alkaline Phosphatase Substrate Kit (Vector Laboratories).

Isolation of primary alveolar macrophages and preparation of conditioned media

Wild-type female SD rats were given 0.5 ml 6% thioglycollate medium (Thioglycollate Medium II, Eiken Chemical Co., Ltd, Tokyo, Japan) by IPS on days 1, 3 and 5, and 6 h after the last treatment, the lungs were excised and minced with sterilized scissors in RPMI 1640 containing 10% fetal bovine serum (Wako Chemicals Co., Ltd) and antibiotics. The homogenate was washed twice and plated onto 6 cm dishes and incubated for 2 h at 37°C, 5% CO₂. The dishes were then washed with PBS three times to remove unattached cells and cell debris. Samples of the remaining adherent cells were cultured in chamber slides and immunostained for CD68 to confirm their identity as macrophages; ~98% of the cells were positive for CD68.

Primary alveolar macrophages were treated with vehicle or TiO₂ particles in saline suspension at a final concentration of 100 µg/ml and then incubated for 24 h in a 37°C, 5% CO₂ incubator. The conditioned medium was collected and diluted 5-fold with RPMI 1640; the conditioned medium had a final concentration of 2% fetal bovine serum.

Western blotting

For the detection of MIP1α, aliquots of 20 µg protein from the extracts of lung or mammary tissue were separated by 15% sodium dodecyl sulfate-polyacrylamide gel electrophoresis, transferred to nitrocellulose membranes and immunoblotted. For the detection of C-C chemokine receptor type 1 (CCR1), 10% sodium dodecyl sulfate-polyacrylamide gel electrophoresis was used for the separation. Membranes were probed overnight at 4°C with anti-rat MIP1α polyclonal antibody (BioVision) diluted at 1:100 or anti-CCR1 (Santa Cruz Biotechnology, Santa Cruz, CA) diluted at 1:100. The blots were washed and incubated for 1 h with biotinylated anti-species-specific secondary antibodies (Amersham Biosciences, Piscataway, NJ) and then visualized using ECL Western Blotting Detection Reagent (Amersham Biosciences). To ensure equal protein loading, the blots were striped with Restore Western Blot Stripping Buffer (Pierce) and re-probed with anti-β actin antibody (dilution 1:2000; Sigma-Aldrich) for 1 h at room temperature.

For the detection of serum MIP1α, GRO and IL-6, aliquots of 150 µg of protein from the sera of rats treated with TiO₂ for 16 weeks were subjected to sodium dodecyl sulfate-polyacrylamide gel electrophoresis. Anti-human GRO polyclonal antibody (BioVision) and anti-mouse IL-6 polyclonal antibody (Santa Cruz) were diluted 1:100. For detection of activated extracellular signal-regulated kinase (ERK) 1/2 and total ERK1/2, phospho ERK1/2 antibody (Cell Signaling Technology, Beverly, MA) and ERK1/2 antibody (Upstate, Lake placid, NY) were diluted 1:2000 and 1:25 000, respectively. The conditioned medium from alveolar macrophages, prepared as described above, was also subjected to western blot assay for MIP1α detection as described above. The blots were striped with Restore Western Blot Stripping Buffer (Pierce) and stained with Ponceau S solution (Sigma-Aldrich) for 10 min. The major band at 66 kDa was judged to be albumin and used as an internal control.

In vitro cell proliferation assay

A549 cells, a human lung cancer cell line, and the rat mammary cancer cell line C3 (19), derived from the *Hras128* transgenic rats, were used in the *in vitro* cell proliferation assays. A549 or C3 cells were seeded into 96-well culture plates at 5 × 10³ cells per well in 2% fetal bovine serum Dulbecco's modified Eagle's medium (Wako Chemicals Co., Ltd). After overnight incubation, the cells were treated as noted below, incubated for 72 h and the relative cell number was then determined.

To investigate the effect of culture supernatant from alveolar macrophages on A549 cell proliferation, their media were replaced with diluted conditioned medium, and the cells were incubated for 72 h with 0, 5, 10 and 20 μ g/ml of anti-MIP1 α neutralizing antibody (R&D Systems, Minneapolis, MN) or with 20 μ g/ml of irrelevant IgG. To investigate the effect of recombinant cytokines on A549 cell proliferation, 10, 50 or 100 ng/ml of recombinant protein, rat MIP1 α (R&D Systems), human GRO (R&D Systems) or human IL-6 (R&D Systems), was added to A549 cells. To investigate the role of ERK in MIP1 α -stimulated cell proliferation, A549 cells, treated with or without 2×10^{-7} M of the specific MAPK/ERK kinase1 (MEK1) inhibitor PD98059 (Cell Signaling Technology) for 10 min, were treated with 50 ng/ml of MIP1 α protein. To investigate the effect of reactive oxygen species (ROS) on cell proliferation, A549 cells, with or without pretreatment with 1 mM *N*-acetyl cysteine (Wako Chemicals Co. Ltd) for 30 min, were treated with 0.5 mM H₂O₂ (Wako Chemicals Co. Ltd). To investigate of the effects of MIP1 α on rat mammary cells, C3 cells were treated with serially diluted recombinant rat MIP1 α (0, 0.4, 2.0, 10 and 50 ng/ml, respectively; R&D Systems). For detecting the direct effect of TiO₂ particles on A549 and C3 cell proliferation, 5×10^3 A549 or C3 cells were cultured overnight and then treated with 10 or 50 μ g/ml of TiO₂ particles.

After 72 h incubation, the relative cell number of A549 and C3 was determined using the Cell Counting Kit-8 (Dojindo Molecular Technologies, Rockville, MD) according to the manufacturer's instruction.

Statistical analysis

For *in vivo* data, statistical analysis was performed using the Kruskal–Wallis and Bonferroni–Dunn's multiple comparison tests. *In vitro* data are presented as means \pm standard deviations. The statistical significance of *in vitro* findings was analyzed using a two-tailed Student's *t*-test and Bonferroni–Dunn's multiple comparison tests. A value of $P < 0.05$ was considered significant. The Spearman's rank correlation test was used to determine the association between TiO₂ dose and TiO₂ carcinogenic activity.

Results

Promoting effects of TiO₂ particles in DHPN-induced lung and mammary carcinogenesis

Prior to initiation of the IPS-initiation–promotion and IPS 9 day studies, we conducted a preliminary study to confirm whether IPS would be a good tool to deliver TiO₂ particles to the alveoli. Rats were treated by IPS with India ink. We observed that ink particles of \sim 50 to 500 μ m in diameter were diffusely distributed throughout the alveoli space (data not shown), confirming that IPS could deliver TiO₂ particles to the alveoli.

Four groups of female *Hras*128 rats were treated with +/- DHPN to initiate carcinogenesis and then treated with TiO₂ by IPS for 12 weeks: Group 1, DHPN alone; Group 2, DHPN followed by 250 μ g/ml TiO₂; Group 3, DHPN followed by 500 μ g/ml TiO₂ and Group 4, 500 μ g/ml TiO₂ without DHPN. Microscopic observation in the lung showed scattered inflammatory foci, alveolar cell hyperplasia (Figure 1A) and adenomas in the DHPN-treated rats. The multiplicity (numbers per square centimeter lung) of hyperplasias and adenomas in Group 3 (DHPN followed by 500 μ g/ml TiO₂) were significantly increased compared with Group 1 (DHPN followed by saline, Table I), and the increase showed a dose-dependent correlation ($\rho = 0.630$, $P = 0.001$ for hyperplasias and $\rho = 0.592$, $P = 0.029$ for adenomas) by the Spearman's rank correlation test. In the mammary gland, TiO₂ treatment significantly increased the multiplicity of adenocarcinomas (Figure 1C) and tended to increase the weight of the mammary tumors (Figure 1C). In the rats, which received TiO₂ treatment without prior DHPN treatment, alveolar proliferative lesions were not observed although slight inflammatory lesions were observed.

TiO₂ was distributed primarily to the lung, but minor amounts of TiO₂ were also found in other organs (supplementary Figure 1A is available at *Carcinogenesis* Online).

Various sizes of TiO₂ aggregates were observed in alveolar macrophages (Figure 1B). The TiO₂-laden macrophages were evenly scattered throughout the lung alveoli. The number of hyperplasias with TiO₂-laden macrophages was dose dependently increased (supplementary Table 1 is available at *Carcinogenesis* Online). This result suggests that TiO₂-laden macrophages may be involved in the promotion of alveolar hyperplasia.

The size distribution of TiO₂ particle aggregate is shown in Figure 1D. Of 452 particle aggregates examined, 362 (80.1%) were nanosize, i.e.

<100 nm. Overall, the average size was 84.9 nm and the median size was 44.4 nm.

IPS 9 day study—analysis of TiO₂

Female SD rats were treated with TiO₂ by IPS over a 9 day period (Figure 2A). Microscopic observation showed scattered inflammatory lesions with infiltration of numerous macrophages mixed with a few neutrophils and lymphocytes in TiO₂-treated animals. Overall, the number of macrophages in the alveoli was significantly increased in the TiO₂-treated animals (Figure 2B). As expected from the results of the IPS-initiation–promotion study, alveolar proliferative lesions were not observed (Figure 2C).

Morphologically, TiO₂ particles were observed as yellowish, polygonal bodies in the cytoplasm of cells (Figure 2D). These cells are morphologically distinct from neutrophils and strongly positive for CD68 (Figure 2E), indicating that the TiO₂ engulfing cells were macrophages. TiO₂ aggregates of various sizes were found in macrophages, and aggregates larger than a single macrophage were surrounded by multiple macrophages (supplementary Figure 1B is available at *Carcinogenesis* Online).

TEM also showed electron dense bodies in the cytoplasm of macrophages (Figure 2F and G). These bodies were found exclusively in macrophages and not found in the alveolar parenchyma, including alveolar epithelium and alveolar wall cells, or in any other cell type. The shape of the electron dense TiO₂ particles in the cytoplasm was quite similar to that observed in preparations taken from TiO₂ suspensions before administration (Figure 2H and supplementary Figure 1C and D is available at *Carcinogenesis* Online). Individual TiO₂ particles were rod-like in shape (supplementary Figure 1C is available at *Carcinogenesis* Online).

Elemental analysis by TEM and X-ray microanalysis indicated that these electron dense bodies were composed primarily of titanium particles (supplementary Figure 1E and F-1 and F-2 is available at *Carcinogenesis* Online). Titanium was not observed in the surrounding alveolar cells without electron dense bodies (supplementary Figure 1F-3 is available at *Carcinogenesis* Online). The size distribution of TiO₂ particle aggregates is shown in Figure 2I. Of 2571 particle aggregates examined, 1970 (76.6%) were <100 nm and five particles were >4000 nm in size. Overall, the average size was 107.4 nm and the median size was 48.1 nm.

IPS 9 day study—analysis of oxidative stress and inflammation-related factors in the lungs of wild-type rats

IPS of TiO₂ particles significantly increased SOD activity (Figure 3A) and 8-OHdG levels (Figure 3B) in the lungs of wild-type rats, but not in the mammary glands. Analysis of the expression levels of 12 cytokines using suspension array indicated that administration of TiO₂ particles significantly upregulated the expression of MIP1 α , GRO and IL-6 in the lung tissue of wild-type rats (supplementary Table 2 is available at *Carcinogenesis* Online). MIP1 α levels were slightly elevated (0.4 pg/mg protein) in the mammary gland (Figure 3C), although the elevation was not statistically significant. Elevation of MIP1 α in the lung tissue of animals treated with TiO₂ particles was confirmed by western blotting (Figure 3D).

Immunohistochemically, MIP1 α was detected in the cytoplasm of alveolar macrophages with phagocytosed TiO₂ particles (Figure 3E upper, stained in red) and these macrophages could be found in hyperplastic lesions of the lung (supplementary Figure 2A and B is available at *Carcinogenesis* Online). MIP1 α was not detected in macrophages without TiO₂ particles (Figure 3E lower). Expression of CCR1, the major receptor of MIP1 α , was observed in the lung; IPS of TiO₂ particles had little or no effect on CCR1 expression (supplementary Figure 2C is available at *Carcinogenesis* Online).

Effect of MIP1 α on proliferation of a human lung cancer cell line *in vitro*

Alveolar macrophages were isolated from the lungs of SD rats and were confirmed to be macrophages by morphology and CD68 staining

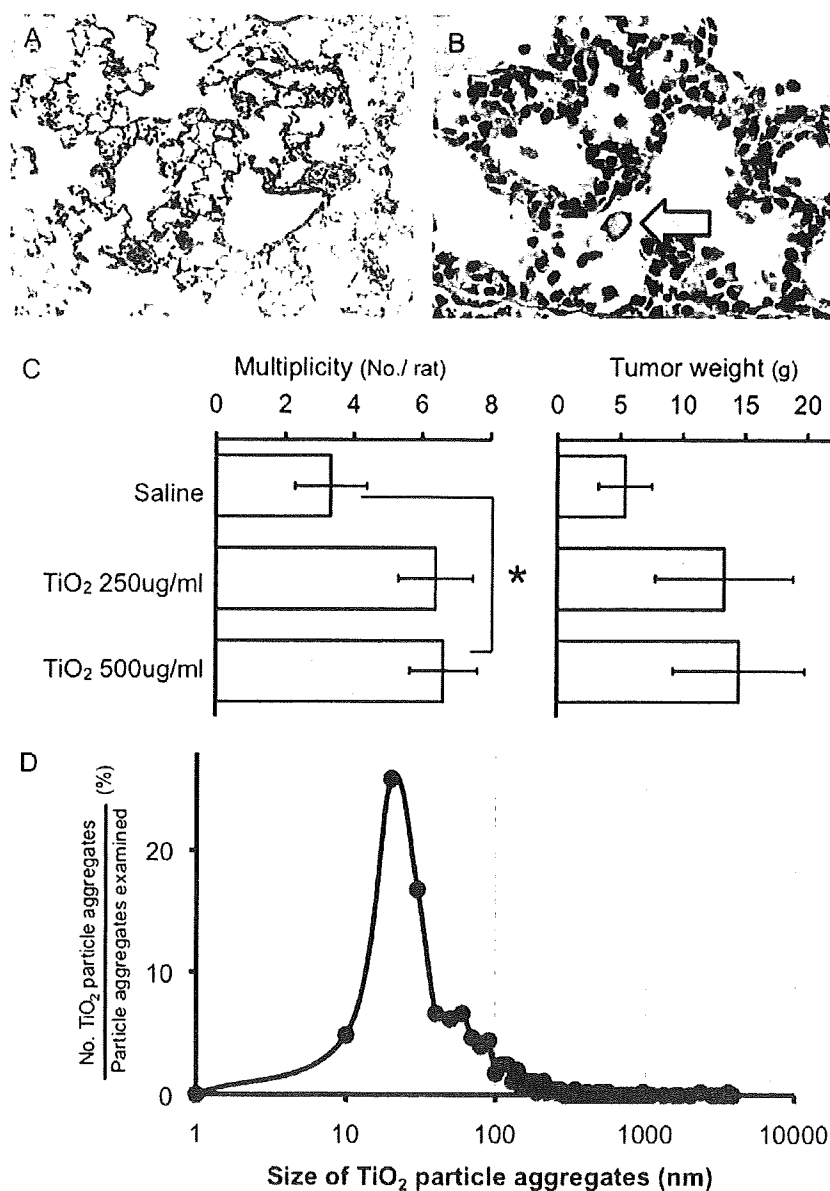


Fig. 1. Promoting effects of TiO₂ particles in DHPN-induced lung and mammary carcinogenesis (A) Alveolar hyperplasias observed in the lung of an *Hras*128 rat receiving DHPN and 500 μg/ml TiO₂ particles. (B) Alveolar macrophages with TiO₂ particles were also observed in hyperplasia lesions. (C) IPS of TiO₂ particles significantly increased the multiplicity of adenocarcinomas in the mammary gland and tended to increase the size of mammary tumors. (D) The size distribution of TiO₂ particle aggregates; among 452 particle aggregates examined, 362 (80.1%) were nanosize, i.e. <100 nm in diameter.

(data not shown). The macrophages were treated with TiO₂ particles suspended in saline (Figure 4A). TiO₂ induced secretion of MIP1α into the culture media (Figure 4B), and the culture medium collected from macrophages treated with TiO₂ particles promoted proliferation of A549 cells, whereas culture media collected from unexposed macrophages did not (Figure 4C). MIP1α neutralizing antibodies attenuated the promotion of A549 proliferation in a dose-dependent manner (Figure 4C). MIP1α-induced cell proliferation was also significantly suppressed by the ERK inhibitor PD98059 (Figure 4D). In addition, MIP1α increased ERK phosphorylation and PD98059 diminished ERK phosphorylation (Figure 4E).

We also examined the effect of MIP1α, GRO and IL-6, H₂O₂ and TiO₂ on the proliferation of A549 cells. MIP1α increased cell proliferation in a dose-dependent fashion, but GRO and IL-6 did not

(supplementary Figure 3A–C is available at *Carcinogenesis Online*). H₂O₂ significantly suppressed cell proliferation, and antioxidant treatment diminished this suppression. Antioxidant treatment did not affect MIP1α-induced cell proliferation (supplementary Figure 3D is available at *Carcinogenesis Online*). These results suggest that ROS have no effect on tumor cell growth in this experiment.

In addition, TiO₂ did not directly increase proliferation of A549 cell (supplementary Figure 3E is available at *Carcinogenesis Online*).

Mechanism analysis of the promotion of mammary carcinogenesis

MIP1α was markedly elevated in the serum of the *Hras*128 rats treated with TiO₂ particles (Figure 5A). Serum levels of IL-6 were not changed by TiO₂ treatment and GRO was not detected in the serum